UNIVERSITY OF HELSINKI

Non-growing season CO_2 fluxes of a boreal fen – key drivers and responses to anomalous winter conditions

Karoliina Särkelä

Master's thesis

Thesis approved in partial fulfilment of a double Nordic Master MSc degree in environmental changes at higher latitudes (EnCHiL), from University of Helsinki and Agricultural University of Iceland.

Supervisors:
Dr. Efrén López-Blanco, Aarhus University
Prof. Timo Vesala, University of Helsinki
Dr. Angelika Kübert, University of Helsinki
Dr. Xuefei Li, University of Helsinki

Helsinki, 17.5.2023

Faculty: Faculty of Science
Degree programme: Environmental Changes at Higher Latitudes
Study track: -
Author: Karoliina Särkelä
Title: Non-growing season CO_2 fluxes of a boreal fen – key drivers and responses to anomalous winter conditions
Level: Master's thesis
Month and year: May 2023
Number of pages: 42 pages, Appendix 3 pages
Keywords: CO_2 fluxes, non-growing season, peatlands, soil temperature
Supervisors: Efrén López-Blanco, Timo Vesala, Angelika Kübert, Xuefei Li
Where deposited: Helsinki University Library
Additional information: Thesis approved in partial fulfilment of a double Nordic Master MSc degree in environmental changes at higher latitudes (EnCHiL), from University of Helsinki and Agricultural University of Iceland.

Abstract:

Non-growing season carbon fluxes can contribute to a significant amount of the full-year ecosystem carbon balance. Year-round net ecosystem exchange (NEE) data from 17 years was used to analyse the non-growing season carbon dioxide (CO_2) fluxes together with environmental and meteorological variables at Siikaneva fen in Southern Finland. Generally, the fen acted as a sink of CO_2 with a mean annual carbon balance of -50.9 (± 39.4) g C m^{-2}. On average, the CO_2 emissions during non-growing seasons offset 57% of the following growing seasons CO_2 uptake. Two years from the 17-year dataset were a consistent net source of CO_2, 2018 and 2016. In 2016, a strong respiration release during the winter-spring transition period turned the annual balance of CO_2 to positive, resulting in the highest emission of CO_2 during the entire study period. The period of anomalous respiration alone offset 38% of the following growing seasons CO_2 uptake. Since the biological activity during non-growing season is low, the CO_2 fluxes likely composed mainly of heterotrophic respiration, and thus were likely driven by soil temperature. The relative importance of air and soil temperature, vapor pressure deficit, water table depth, and photosynthetically active radiation (PAR) on NEE of CO_2 was analyzed with a random forest algorithm. PAR and soil temperature were the most important drivers during non-growing season, growing season and year-round periods. PAR had the highest importance during growing season while during non-growing seasons, PAR and soil temperature had an equal relative importance. A wavelet coherence analysis further revealed that the mean annual cycles of NEE and soil temperature were coherent during the summer months across the diurnal scale. For instance, NEE correlated positively (decreasing the net carbon sink) with soil temperature and lagged the response to temperature by 4-6 hours. There was no coherence between the annual cycles of soil temperature and NEE during winter. The results emerging from this thesis stress the importance of studying what controls the interannual variation in soil temperature and the possible accumulation of CO_2 in soil during non-growing season, but also how they contribute to spring-time CO_2 releases like the one observed in spring 2016.

Table of contents

1 Introduction

Boreal and sub-arctic peatlands are one of the world's largest terrestrial carbon pools, with estimates ranging from 400 - 600 Gt of carbon (Gorham, 1991; Yu et al., 2011) to 1000 Gt of carbon (Nichols & Peteet, 2019). Even with the conservative estimates, boreal and sub-arctic peatlands account for 30% of the global soil carbon pool (Friedlingstein et al., 2022). Increased soil respiration triggered by global warming could strengthen the release of such large amount of carbon stored in soils (Bond-Lamberty et al., 2018), causing a positive feedback to the atmosphere further accelerating global warming (Frey et al., 2013). There are high uncertainties in the magnitude of the soil-climate feedback (Bradford et al., 2016), with the greatest uncertainties found in northern latitudes (Warner et al., 2019).

High latitudes are warming over three (Arctic Monitoring and Assessment Program [AMAP], 2021) to four (Rantanen et al., 2022) times as fast as the global average. Likewise, winters are observed (AMAP, 2021; Mikkonen et al., 2015) and projected (Intergovernmental Panel on Climate Change [IPCC], 2022) to warm faster than any other period throughout the year. Warming during winter can intensify microbial processes and thus increase the amount of carbon emitted via heterotrophic respiration (López-Blanco et al., 2018; Natali et al., 2019).

The winter carbon cycle is dominated by the ecosystem respiration processes and is primarily controlled by soil temperature (Natali et al., 2019; Curiel Yuste et al., 2007). Soil temperature during wintertime is controlled by both the ambient air temperature and the insulating effect from the snowpack. The projected increase in temperature and decrease of snowfall (AMAP, 2021; IPCC, 2022) will thus very likely have contrasting impacts on the temperature conditions along the soil profile. The reduction in snow cover, even with generally warmer temperature during winter, may lead to colder temperatures at the soil surface in the future (Groffman et al., 2001). However, the warming could be enhanced at the deeper soil layers due to generally warmer air temperature throughout the year: once warmed, the deeper layers have found to retain the heat longer, while the surface layer can get cooler without the insulating effect of snow (Qian et al., 2011). Wintertime carbon fluxes could therefore be exposed to these two competing processes in the future driven by changes in climate forcing.

Currently, the wintertime carbon flux observations are poorly understood, scarce and underrepresented compared to summertime observations (Virkkala et al., 2022). In the ABCFlux database (Virkkala et al., 2022), a comprehensive dataset including data from 244 stations that focuses on carbon fluxes from boreal and arctic ecosystems, only 18 % of the observations cover the winter months. Out of all the observations from all the sites at the database, the annual carbon budgets can be calculated for only 267 site-years (Virkkala et al., 2022). This recent synthesis effort points to an important knowledge gap and why long, year-round datasets of ecosystem carbon dynamics are valuable for understanding the ecosystem processes across seasons that shape the annual carbon balance and its associated sensitivity. Ignoring the wintertime fluxes can lead to severely overestimating the annual carbon sink (Aurela at el., 2002), and thus accounting for the non-growing season cumulative carbon budget of the year-round carbon balance is crucial to reliably understand the sink-source potential of northern ecosystems. To address the uncertainties in the terrestrial carbon cycle (Arora et al. 2020; Friedlingstein et al., 2022), increased understanding of the non-growing season carbon fluxes is critically needed.

Recent studies suggest that the winter conditions, such as changes in soil temperature and presence of snow or ice, can potentially have carry-over effects in the respiration events during spring in the time of snow melt and soil thawing. A small number of studies has observed bursts of carbon dioxide (CO_2) during spring-thaw periods, highlighting the importance to study these rarely observed events (Arndt et al., 2020; Mastepanov et al., 2013; Raz-Yaseef et al., 2017; Yu et al., 2010; Wang et al., 2023). Even if not frequent in time, the magnitude of such pulses can reduce the annual carbon uptake by 46% (Raz-Yaseef et al., 2017), and therefore contribute greatly to the annual carbon balance. In fact, a period of anomalously high respiration has also been found in Siikaneva fen in Spring 2016. There are various processes that can lead to these pulses of emissions. For instance, snow and ice can act as a physical barrier between the soil and atmosphere, resulting in the accumulation of winter-time CO_2 emissions in soil and snowpack that may later be released into the atmosphere (e.g. Sullivan et al., 2012). Furthermore, the thawing of soil after freezing can trigger an increase in microbial respiration (Schimel & Clein, 1996).

To understand the role of wintertime periods on the overall year-round carbon balance, this thesis analyses an extensive time series dataset covering the 2005-2021 period from Siikaneva fen. Siikaneva fen is a long-term Eddy Covariance measurement site with year-round measurements in southern Finland. The dataset used in this thesis is unique in its temporal coverage both in length and in terms of measurements including wintertimes. The 17 years of year-round net ecosystem exchange (NEE) observations from Siikaneva fen accounts for 6% of all the site-years with year-round data from 244 sites included in the ABCFlux database (Virkkala et al., 2022). The net ecosystem exchange (NEE) of CO_2 data from Siikaneva fen has been previously studied in four studies, covering data from 2005 to 2015 and the year 2018. The NEE during the 2004 to 2005 period was studied by Aurela et al. (2007). The NEE from 2006 to 2008 was compared to a northern fen site by Aurela et al. (2009). Rinne et al. (2018) studied the relationship between methane and NEE of CO_2 for the period of 2005-2015. The impact of a drought period to the NEE in summer 2018 was analyzed by Rinne et al. (2020).

The aim of this study is to analyze the non-growing season dynamics of NEE and soil temperature and their overall impact to the annual CO_2 balance, and to study the conditions during the respiration event in spring 2016. I hypothesize that soil temperature is a key driver of NEE during the non-growing seasons. Additionally, I expect that soil temperature leads the NEE, meaning that there is a lag between them. I hypothesize that the lag is longer during winter due to the insulating effect of snow cover. To address these hypotheses, I ask the following research questions:

1. How much does the non-growing season carbon balance account for the whole annual carbon balance?
2. What is the relationship between soil temperature and NEE and to what extend does soil temperature drive the carbon exchange across seasons?
3. What were the meteorological and environmental conditions before and during the anomalous winter-spring transition period in 2016, and how much did it contribute to the overall annual net carbon balance?

2 Background

2.1 Ecosystem scale carbon fluxes and the Eddy Covariance method

The CO_2 cycles between the ecosystem and atmosphere by two competing fluxes, photosynthesis and respiration. Gross primary production (GPP) is a measure of CO_2 fixed in photosynthesis per unit time at an ecosystem level, while ecosystem respiration (Reco) refers to CO_2 released by decomposition and metabolic processes of both autotrophs and heterotrophs (Chapin et al., 2011, p. 210). The Net Ecosystem Exchange (NEE) is the net balance between these two competing gross fluxes, i.e., GPP and Reco, and it indicates the net CO_2 balance between ecosystem and atmosphere. The sign convention used in this thesis uses negative values to represent a net CO_2 uptake and positive values to characterize net CO_2 emission. GPP, Reco, and NEE typically follow a well-defined annual cycle, with the highest GPP and Reco occurring in summer due to optimal environmental conditions for photosynthesis and biological activity (Chapin et al., 2011, p. 210). Despite the peak Reco in summer, photosynthesis usually offsets the emission outputs, resulting in a negative NEE, i.e., a net sink of CO_2 (Chapin et al., 2011, p. 210). During winter, however, a lack of photosynthesis results in a positive NEE, despite the lower Reco levels compared to the summer period (Chapin et al., 2011, p. 210).

The NEE of CO_2 can be measured with the Eddy Covariance (EC) technique, which is used to quantify the exchange of energy, mass, and momentum between a surface and the atmosphere (Aubinet et al., 2012, p. 1). The atmosphere contains turbulent motions, referred to as eddies, that transport trace gases such as CO_2 between the surface and atmosphere. The vertical flux between the surface and atmosphere can be determined by calculating the covariance of the vertical wind velocity and concentration of CO_2. This method can be applied continuously over large, preferably homogenous and flat areas, providing a whole-ecosystem scale CO_2 balance at very high temporal resolution (Baldocchi et al., 2003). The measured NEE can be partitioned into GPP and Reco by using different statistical models, which can be further used to fill data gaps. Since GPP and Reco are eventually model outputs and not true observations, they bring unavoidable uncertainty to analysis featuring them. Thus, analysing them and the gap-filled data based on them should be done with care to avoid circularity issues since they are based on environmental variables (e.g PAR and air temperature).

2.2 Winter conditions impact on soil temperature and the soil efflux

During winter, plants are not photosynthetically active and generally the biological activity is low (Chapin et al., 2011, p. 210). However, microbes can remain active below freezing temperatures (Panikov et al., 2006), in boreal soil likely at least until -9 °C (Martz et al., 2016). Therefore, the winter-time carbon fluxes are comprised mostly of heterotrophic respiration. Even though the positive fluxes are generally small during winter, the long duration of the cold period in high latitudes can significantly contribute to the annual carbon balance (Natali et al., 2019; López-Blanco et al., 2018).

Heterotrophic respiration is mostly regulated by temperature and moisture in soils (Chapin et al. 2011, p. 192). During the cold season, soil temperature is affected by both the ambient air temperature and the presence of snow. Snow insulates the soil from cold air, and a snowpack of 40 cm deep can fully decouple soil temperature from the air temperature (Zhang, 2005). Snow can thus sustain warmer temperatures, and therefore by preventing water from freezing, also moister conditions in soil. Snow cover can thus enhance the conditions for microbial activity in the soil and as a result, maintain higher respiration rates than with lower snow depth (Morgner et al., 2010).

Climate change is expected to decrease the depth and duration of snow cover in most regions at high latitudes in the future (AMAP, 2021). As a consequence, with less snow to insulate the ground the soil temperatures at the surface could be colder during the winter compared to ambient conditions (Groffman et al., 2001). A decrease in soil temperature could ultimately result in lower soil carbon efflux even though generally winters would get warmer.

However, without the insulating effect over ground from the snowpack, soil temperature can fluctuate with air temperature, which could lead to cycles of soil freezing and thawing if the air temperature fluctuates below and above 0 ◦C. Freeze-thaw cycles can have contrasting impacts on the soil microbes and thus on the respiration (Li et al., 2021). Freezing of soil can kill some microbial communities, but as a consequence, a large amount of easily decomposable carbon and nutrients becomes available in the soil, which in turn favors the remaining communities (Brooks et al., 2005). This process can promote a pulse of respiration during soil thaw (Schimel & Clein et al., 1996). However, these pulses get smaller in magnitude with repetitive freeze-thaw cycles (Schimel & Clein et al., 1996; Li et al., 2021). The changing conditions affect the microbial species composition in the soil, which results in higher species richness after freeze-thaw cycles, and altered temperature and moisture sensitivity since cold-tolerant microbes are adapted to colder and drier conditions (Aanderud et al., 2013). This means that the freeze-thaw cycles have largest impact when the microbial communities are not adapted to them. These pulses of respiration associated with freeze-thaw cycles could offset some of the decreased soil carbon efflux caused by colder soils.

Besides of controlling the soil temperature, snow and ice can act as a physical barrier between the surface and atmosphere, which can cause the respiratory fluxes to accumulate in the soil (Martz et al., 2016; Morgner et al., 2010). This accumulated respiration is then later released back to the atmosphere when soil thaws, causing a lag between the changes in soil temperature and the respiration flux to the atmosphere (Sullivan et al., 2012). Therefore, snow cover affects both the rate of the respiration and the temporal dynamics of it. Changing conditions in snow cover can thus cause interannual variation in temporal dynamics in the observed CO_2 fluxes. A lag between changes in environmental variables like soil temperature and measured fluxes creates a challenge when assessing how these variables control the fluxes.

3 Methods

3.1 Site description

Siikaneva wetland is an oligotrophic fen located in southern Finland (61°50N, 24°12E, 162 m above sea level). The measurements at the site have been ongoing since 2005. The site has been part of the ICOS research infrastructure since 2017 and is a class 2 ecosystem station. The peat depth varies from 2-6 meters at the site. The site has no permafrost. The surface is generally flat, and the vegetation is dominated by peat mosses (*Spaghnum balticum* [Russow] C.E.O. Jensen, *S. majus* [Russow] C.E.O. Jensen, *S. papillosum* Lindb.), sedges (*Carex rostrata* Stokes, *C. limosa* L., *Eriophorum vaginatum* L.) and Rannoch rush (*Scheuchzeria palustris* L.) (Rinne et al., 2007). The site is surrounded by a Scots pine forest. The mean annual temperature during 1971-2000 was 3.3 ◦C and annual total precipitation 713 mm at Hyytiälä weather station, located 5 km from Siikaneva (Drebs et al., 2002).

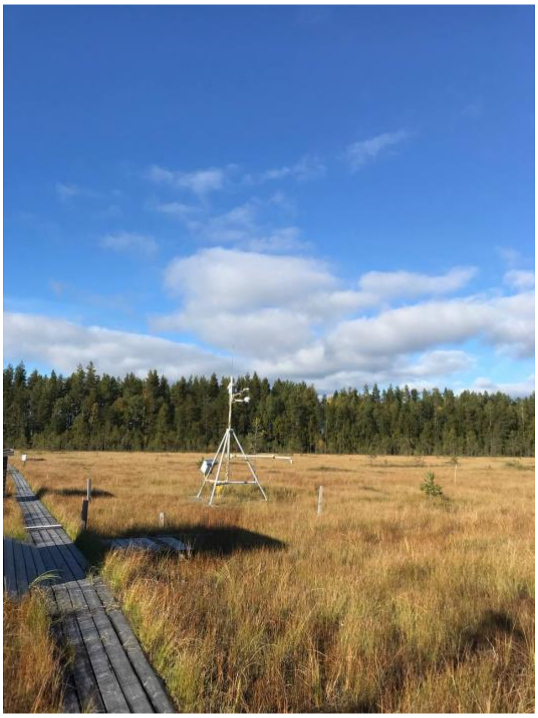

Picture 1. Siikaneva in September 2022, including the Eddy covariance tower in the middle. Photo by Maximilian King.

3.2 Definition of non-growing season and growing season

Dividing the year into conventional seasons like winters and summers can be challenging due to the lack of set definitions, and inherent inter-seasonal variability. Instead, terms like growing season and non-growing season can be used to define the period in the year when plants are able to grow, since these terms captures the impact of what location-specific climatic conditions have on ecosystem processes. The distinction between non-growing season and growing seasons lacks a standardized definition. Different definitions can be used that are based on environmental variables such as air temperature or presence of snow cover (Arndt et al., 2020; Rafat et al., 2022), or seasonality derived from GPP information (Böttcher et al., 2014). In this study, I use the terms growing season (GS) and non-growing season (NGS) to refer to the parts of the year when the ecosystem is a net carbon sink (GS) and a net carbon source (NGS), based on the daily values of NEE (Aurela et al., 2004). I chose the GS definition based on NEE information to avoid circularity issues from further analyzing different forcing variables controlling NEE between the two seasons. The chosen definition divides the year into only two seasons and does not make a distinction between the shoulder (autumn and spring) seasons.

The first day of the GS was defined as the first day of three consecutive values of negative NEE and similarly, the last day of GS as the first day of three consecutive values of positive NEE, following a definition for sink period presented by Aurela et al. (2004). NGS started when the GS ended and, similarly, ended when the next GS started.

3.3 Eddy covariance (EC) measurements

Picture 2. Eddy covariance mast in July 2022 (left, photo by Maximilian King) and March 2023 (right, photo by Eyrún Gyða Gunnlaugsdóttir).

The NEE of CO_2 observations have been measured in Siikaneva since 2005, although there was a major instrumentation upgrade in late 2015. The instruments used between 2005 and 2015 were Metek USA-1 anemometer (Metek GmbH, Elmshorn, Germany) and LI-COR LI-7000 gas analyzer (LI-COR, Lincoln, NE, United States). In 2016-2021 the instruments used were Gill HS-50 anemometer (Gill Instruments Ltd., England, United Kingdom) and LI-COR LI-7200 gas analyzer (LI-COR, Lincoln, NE, United States). The flux tower was set up at 2.7 m height. The change of the instrumentation caused an unavoidable gap in the time series from September 2015 to February 2016.

The NEE data has been filtered with turbulence intermittency and atmospheric stability, corrected by CO_2 storage flux and subsequently gap-filled. The data was readily available at SmartSMEAR database upon the start of the thesis (https://smear.avaa.csc.fi/download). In case of missing data, NEE was calculated as the sum of modelled GPP and Reco. GPP was modelled with site- and time-specific parameters using PAR and air temperature. GPP was forced to zero during air temperatures below 0 °C. Reco was modelled by using site- and time-specific parameters based on air temperature. The respiration function used air temperature instead of soil temperature due to the inconsistent soil temperature time series at the site. On other parts, the method follows the process described in Kulmala et al. (2019). Pre-processed and gap-filled hourly averaged NEE data was further aggregated into daily sums and converted from micromoles of CO_2 to grams of carbon. The fluxes are expressed from the perspective of the atmosphere: negative flux indicating net carbon uptake and positive sign indicating net carbon efflux.

3.4 Ancillary measurements

Soil temperature was measured with Campbell 107 thermistor (Campbell scientific, inc., Logan, UT, United States) between 2005 and 2016. Soil temperature was measured at two microsites at Siikaneva in 2005-2016 (named hummock and lawn microsite at the SmartSMEAR database). I used data measured at the lawn site since it represents the footprint area around the EC tower. During 2017-2021 the soil temperature was measured with UMS TH3-s temperature profile probe (UMS GmbH & Co. KG, Willmars, Germany) and was an average of five microsites inside the EC footprint area. I used data measured at 5 and 50 cm depths for 2005-2016 and 5 and 45 cm depth for 2017-2021. From hereafter, the temperature measured at either 50 cm or 45 cm depth is referred to as “soil temperature at 50 cm depth”.

Photosynthetically active radiation (PAR) was measured with Li-Cor Li-190R quantum sensor (LI-COR, Lincoln, NE, United States). The data for years 2009-2015 were excluded due to instrument malfunction.

Air temperature and relative humidity were measured with Rotronic HC2 sensor (Rotronic AG, Bassersdorf, Switzerland). I then calculated vapor pressure deficit (VPD) with a function fCalcVPDfromRHandTair from an R package Reddyproc (Wutzler et al., 2022) that calculates VPD from relative humidity and air temperature. VPD describes the deficit between the amount of vapor that the saturated air can hold at a current air temperature and the observed amount of water vapor currently in the air.

Water table depth (WTD) was measured with Druck PDCR1830 (Campbell scientific, inc., Logan, UT, United States) and Campbell CS451 pressure transducer (Campbell scientific, inc., Logan, UT, United States). WTD is expressed as height of the water table from the surface, negative value referring to a WTD below surface.

Precipitation was measured with ARG-100 tipping bucket rain gauge (Campbell scientific, inc., Logan, UT, United States) for 2005-2016. The instrument does not reliably detect sleet or snow. In 2017 the instrument was changed to OTT Pluvio2S weighing rain gauge (OTT HydroMet, Kempten, Germany).

Many of the instrumentations were renewed in late 2015, causing a gap in the measurements for most of the variables. The duration of the gap differs between the variables. To gain better understanding of the conditions in the autumn and winter 2015, air temperature and snow depth data was reviewed from Hyytiälä forestry station, which is located 5 km from Siikaneva. At Hyytiälä, the air temperature was measured with Pt100 sensor inside a custom shield. A linear regression model with air temperatures from the two stations had a coefficient estimate close to 1 (0.98) and an R-square of 0.98, which validated using the air temperature data from Hyytiälä. However, the snow depth varied between the stations, and thus interpreting Hyytiälä snow depth as a proxy for snow condition in Siikaneva should be taken as indicative only.

3.5 Wavelet coherence analysis

Wavelet coherence analysis is a method to identify significant relationships between two time series over different periods (Grinsted et al., 2004). Coherence is a measure similar to correlation, that is used in time series analysis to detect similarities between local oscillations (i.e., waves) in two time series. Wavelet coherence analysis can be used to identify these correlating oscillations and to quantify the temporal difference, or a lag, between them. I explicitly used wavelet coherence analysis to study whether there was coherence between the average annual cycles of NEE and soil temperature, if the coherence was different between NEE and soil temperature at 5 cm and 50 cm depth, and if there was a lag between them that would change seasonally. I aggregated all years together to calculate an average value for each hour of each day. The average hourly values for day of year (DoY) 1-366 thus represented typical oscillations or patterns that occur yearly. I separately conducted the analysis between NEE and soil temperature measured at 5cm and 50 cm depth, respectively.

Spring 2016 was found to have anomalous dynamics both in NEE and soil temperature at depth 50 cm. Thus, I additionally performed a similar analysis between NEE and soil temperature measured at 50 cm depth for the year 2016 independently, to study the level of coherence between them. I then compared the results for 2016 to a wavelet coherence analysis of the mean values of the complete time period excluding the year 2016. There was a gap in the data for DoY 188-246 for soil temperature at 50 cm depth in 2016. I gap-filled the missing data using a transition function based on functions from two linear regression models that used soil temperature at 50 cm depth measured at Hyytiälä site to model the missing temperature data at a corresponding depth from Siikaneva. One of the models were trained with 50 days of data before the gap and the other with 50 days of data after the gap. I then used a function that incrementally changed at each time step from the function obtained from the model for before the gap to the function obtained from the model for after the gap (Appendix 2 Fig. A2). The adjusted R-squares were 0.94 for the model before the gap (for DoY 138-187) and 0.99 for the model after the gap (for DoY 247-296).

3.6 Random forest

Random forest is a machine-learning algorithm used for complex multi-regression (e.g. López-Blanco et al., 2017) and classification (e.g Rudd et al., 2021) data analyses. In this thesis I used random forest to quantify the relative variable importance of different environmental drivers controlling the carbon sink or source strength (i.e., NEE). Random forest creates multiple decision trees that use different random subsets of the training data (Breiman, 2001; Pedregosa et al., 2011). The random forest classifier partitions explanatory variables (covariates) into groups, and for each resulting cluster, a multiple linear regression model is constructed to predict NEE (response variable) based on the corresponding driving factors. The variable importance is expressed as the fraction (percentage, 0-100%) of decisions in which the variable is used for clustering the data in ratio to all decisions. This analysis used PAR, VPD, soil temperature, WTD and air temperature to explain the variability of NEE. I assessed the variable importance over the whole period of 2005-2021. Additionally, I partitioned the time series into NGSs and GSs to explore how the variable importance varies between these seasons.

This analysis does not include precipitation data as explanatory variable since the instrument measuring precipitation was not able to reliably detect snow and sleet. Therefore, such data could introduce biases in the analysis by underestimating the amount of precipitation during winter (aggregated to NGS) compared to summer (aggregated to GS). Although precipitation is an important factor in climate variability, including precipitation as a covariate in the random forest analysis could have created artifacts due to the consistent uncertainty in the dataset between NGSs and GSs.

3.7 Data analysis

I analyzed the data in RStudio (version 4.1.1, 10.8.2021). Wavelet coherence analysis was done with a package Biwavelet (Tarik et al., 2021). I used packages ggplot2 (Wickham, 2016) and gridextra (Auguie, 2017) for the data visualization. For general processing and gap-filling, packages dplyr (Wickham et al., 2021) and imputeTS (Moritz et al., 2017) were used. VPD was calculated with a function fCalcVPDfromRHandTair from package REddyProc (Wutzler et al., 2022). For random forest analysis I used Python language (version 3.8.6rc1). I used RandomForestRegresso-function from sklearn library (Pedregosa et al. 2011) for the random forest analysis. Additionally, I used libraries NumPy (Harris et al., 2020) and matplotlib (Hunter, 2007) for general data wrangling and exploration.

4 Results

4.1 Duration of NGS

On average, 60% of the year was part of the NGS. NGS started on average on September 17th (DoY 260 ±19) and ended on April 30th (DoY 120 ±15), lasting on average for 226(±27) days (Fig. 1).

NGS started latest in 2011 on October 26th and earliest in 2018 on July 30th (Fig. 1, in figure the years 2012 and 2019). NGS ended the earliest in 2006 on March 18th and latest in 2016 on June 2nd. The NGS that started in 2018 and ended in 2019 was the longest NGS (278 days) in the whole study period due to an exceptionally early start of the season (Fig.1, in figure the year 2019). Similarly, the early end of the NGS in 2006 resulted in the shortest (162 days) NGS in the study period.

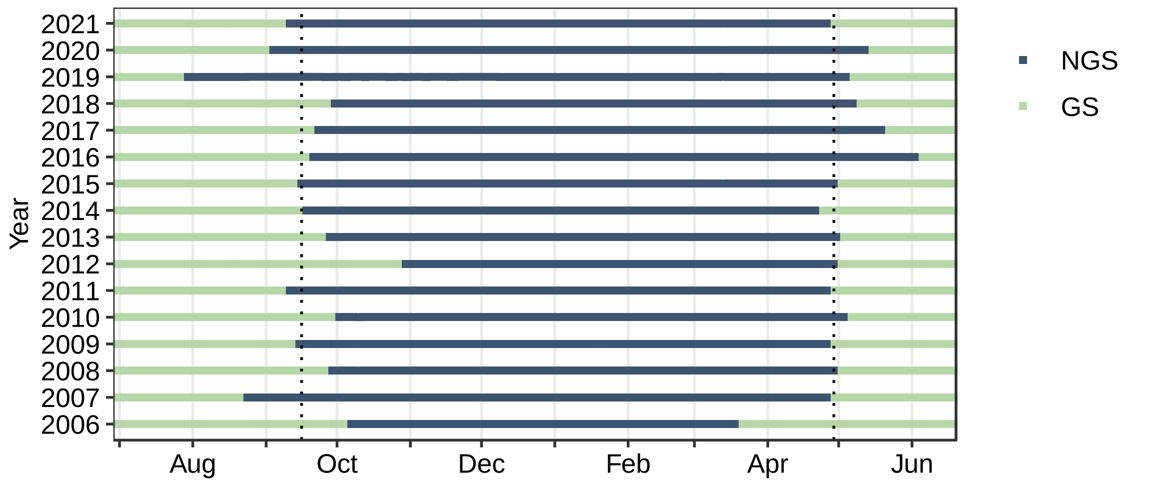

Figure 1. Non-growing season (NGS) and growing season (GS) in years 2005-2021. Year on the y axis refers to the year starting in January. The dashed line on the left represents the DoY when the NGS started on average (DoY 260, September 17th) and the dashed line on the right the DoY when the NGS ended on average (DoY 120, April 30th).

4.2 Ancillary information

4.2.1 Meteorological variables, water table depth and snow depth

The mean temperature for the whole time period was -1.5 ◦C during NGS and 12.9 ◦C during GS (Fig. 2A). The mean precipitation during GS was 250 mm and 242 mm measured with the ARG-100 tipping bucket rain gauge for 2005-2016 and the OTT Pluvio2S weighing rain gauge for 2017-2021, respectively (Fig. 2C). The mean precipitation during NGS was 200 mm in 2005-2016 and 350 mm in 2017-2021 (Fig. 2C) with similar instrumentation set up, respectively. The precipitation in NGS's in

2005-2016 was lower than NGS's in 2017-2021 since ARG-100 tipping bucket rain gauge does not detect snow or sleet (Fig 2C). Daily PAR was 68 µmol $m^{-2}s^{-1}$ in NGS and 314 µmol $m^{-2}s^{-1}$ during GS (Fig. 2B). The mean WTD was higher during NGS (-3.6 cm) than in GS (-10.5cm, Fig. 2E). Vapor pressure deficit was 0.07 kPa during NGS and 0.4 kPa during GS (Fig. 2D). There was on average 150 days of snow on the ground (snow depth > 0 cm) during the NGS's, with mean snow depth varying from 3.0 cm in NGS that started in autumn 2016 to 28 cm in NGS that started in 2020 (Fig. 2F).

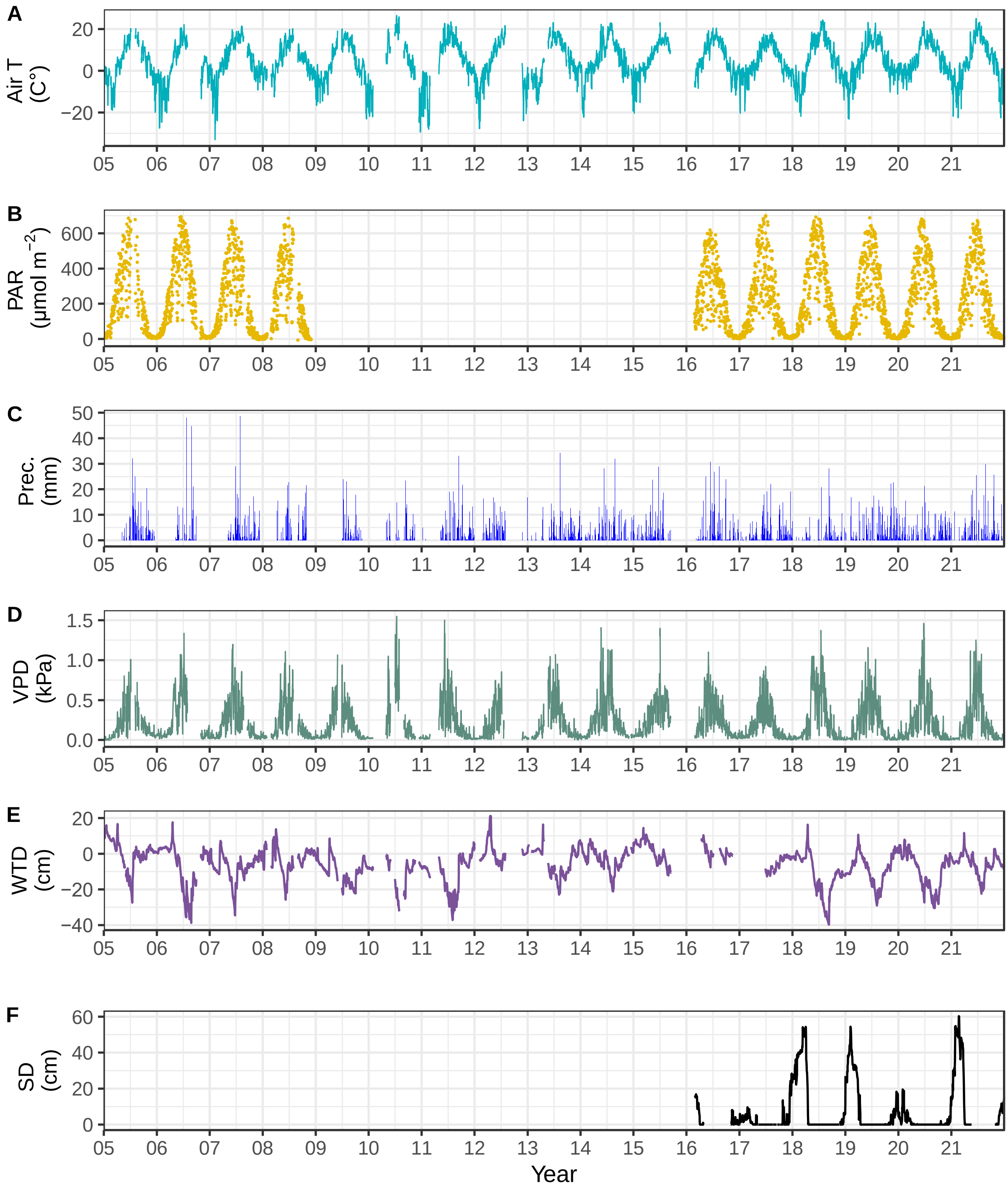

Figure 2. Time series of air temperature (**A**), precipitation (**B**), photosynthetically active radiation (**C**), vapor pressure deficit (**D**), water table depth (**E**) and snow depth (**F**) in 2005-2021. Precipitation is expressed as daily sums and is calculated from the hourly summed data. The other variables are expressed as daily means and are calculated from hourly averaged data. Data for PAR in 2009-2015 was not used due to instrument malfunction. Snow depth measurements started at spring 2016. Precipitation data shown in the figure is measured with ARG-100 tipping bucket rain gauge in 2006-2016 and with OTT Pluvio2S weighing rain gauge in 2017-2021.

4.2.2 Soil temperature

The soil was colder at the surface (2.4 ◦C at 5 cm) than at deeper layer (4.7 ◦C at 50 cm) during NGS, and warmer at the surface than at deeper layers during GS (12.9 ◦C and 10.9 ◦C at 5 and 50 cm depth, respectively, Fig. 3). The annual mean soil temperature was 6.5 ◦C and 7 ◦C at 5 and 50 cm depth, respectively. The coldest surface temperature (-0.76 ◦C) was measured in January 2016 (Fig. 3). A similar peak in soil temperature was not found in other years (Fig. 3).

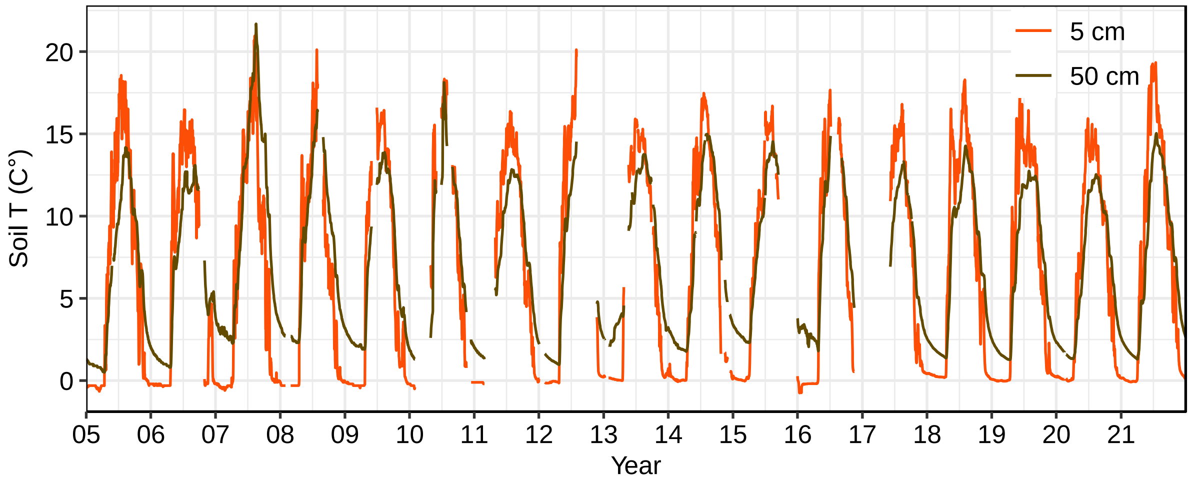

Figure 3. Time series of daily means of soil temperature at 5 cm depth (red line) and 50 cm depth (brown line). Daily means are calculated from hourly averaged data. The measurement practices changed in 2017, including the measurement depth. The figure of the time series of soil temperature at 50 cm depth includes the temperature measured at 50 cm depth for 2005-2016 and temperature measured at 45 cm depth for 2017-2021. The data for both measuring depths is from lawn microsite for 2005-2016 and an average of five microsites for 2017-2021.

At the surface, soil temperature dropped below 0 ◦C in 15 years out of 16 (Fig. 4. For the winter 2016 to 2017 there was no available data, year 2017 in the figure). At 20 cm depth, the soil temperature dropped below 0 ◦C across 7 years (Fig. 4). Based on the available data, on average the soil stayed below 0 ◦C for 66 days at 5 cm depth and 17 days at 20 cm depth. However, there were long periods of missing data (Fig. 4). In 2005, it is likely that the soil temperature dropped below 0 ◦C before the period of available data, because the soil temperature was already below 0 ◦C at 20 cm depth during the first measurements (Fig. 4). Also, it is likely that the soil stayed longer below 0 ◦C in 2010 and 2011, and through the period of missing data in the middle of the winter 2008 (Fig. 4). Despite this bias that underestimates the duration of soil temperature below 0 ◦C for the earlier years in the study period, there was a decreasing trend in the duration of soil T below 0 ◦C at 5 cm depth (correlation -0.61).

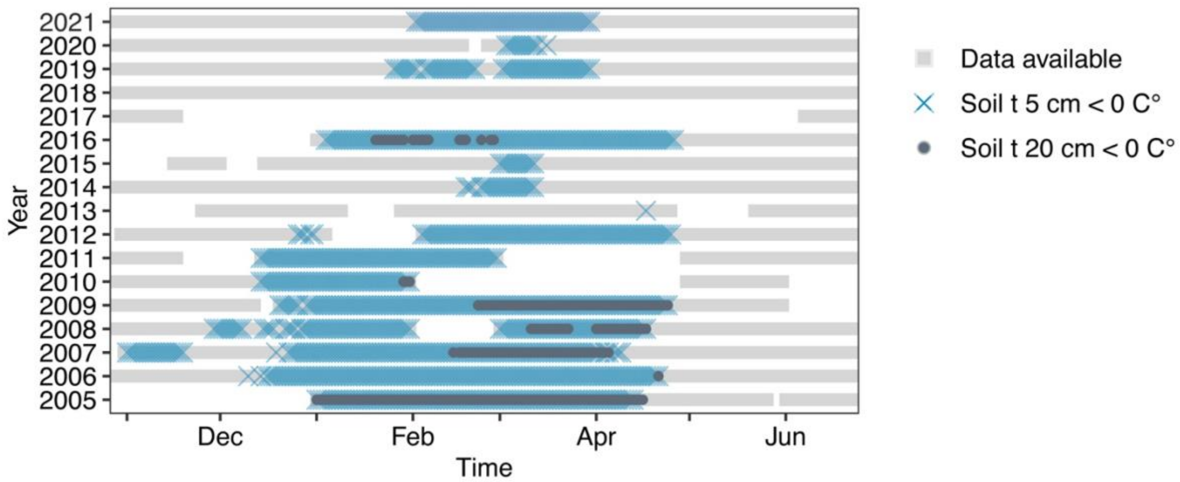

Figure 4. Days of daily mean soil temperature below 0◦C at 5 cm (light blue) and 20 cm (dark blue) depth. Year on the y axis refers to the year starting in January. Data availability of soil temperature is marked as light grey.

4.3 CO_2 fluxes

4.3.1 Annual fluxes and balances

The annual carbon balance (the cumulative sum of the daily NEE for the period of DoY 1-365 and DoY 1-366 in leap years) was -50.9 ± 39.4 g C m^{-2}, meaning that during the whole study period, on average the fen acted as a net carbon sink. The annual balances ranged from -105.4 g C m^{-2} in 2012 to 28.4 g C m^{-2} in 2016 (Fig. 5B). In addition to the year 2016, the fen was a source of carbon in 2018, with annual balance of 21 g C m^{-2} (Fig. 5B). In the whole study period across the 2005-2021 period, the daily NEE varied from -2.8 to 1.49 g C m^{-2} (Fig. 5A), with the mean of -0.13 ± 0.6 g C m^{-2}. Throughout the whole period the fen fixed 866 g C m^{-2} in total.

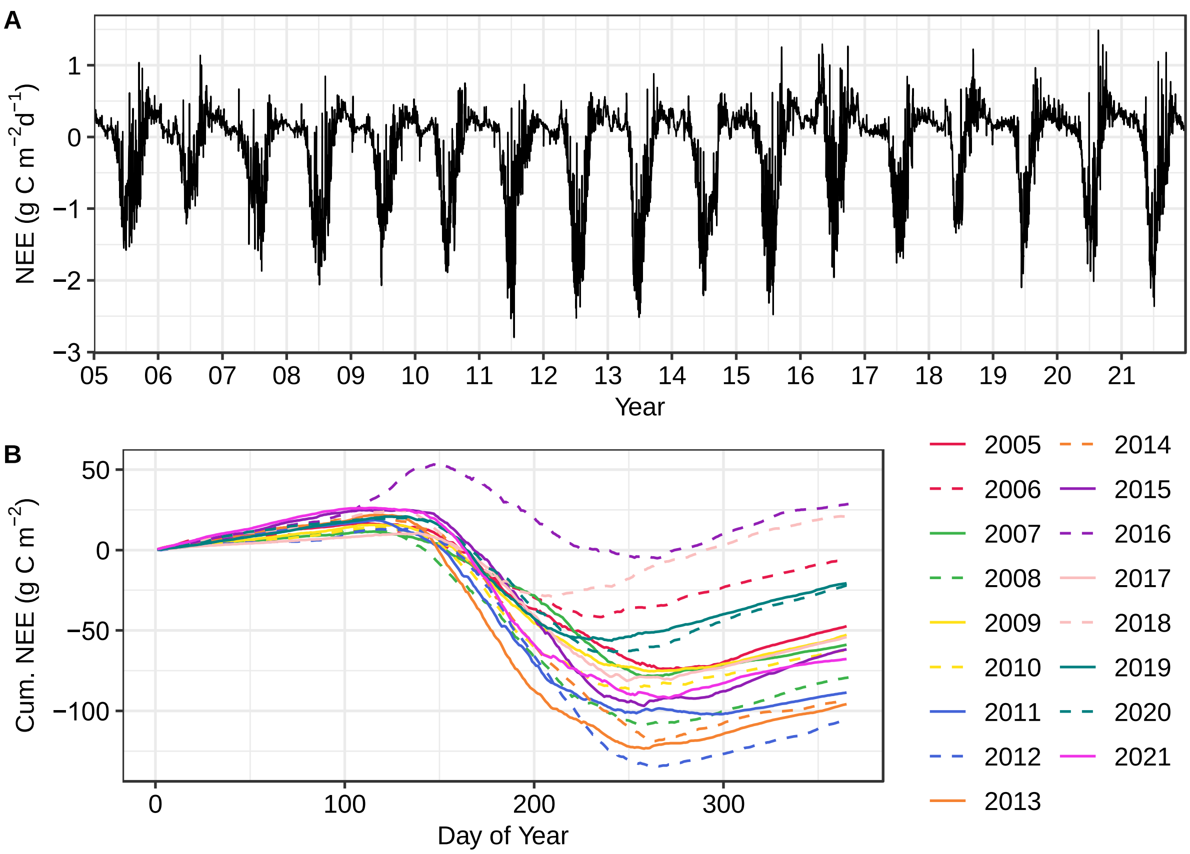

Figure 5. Time series of daily sums of gap-filled NEE for 2005-2021 (**A**) and the cumulative annual sum (**B**) of NEE for DoY 1-365 and 1-366 for leap years. Daily sums are calculated from hourly averaged data.

4.3.2 NGS CO_2 fluxes

The mean cumulative carbon balance during NGS was 49.37 (±15.05) g C m^{-2}. The year 2012 had the lowest cumulative carbon balance over the NGS and 2016 the highest, releasing 26 g C m^{-2} and 84.4 g C m^{-2}, respectively (Fig. 6). On average, 57% of the growing season's carbon uptake (-99.75 ± 30.58 g C m^{-2}) was offset by the previous emissions during the NGS. However, there was high variability between the years (± 33%). Both the duration of the NGS and the daily fluxes correlated equally well with the cumulative sums (duration 0.73, mean daily values 0.77). The mean daily CO_2 flux was 0.21 (±0.048) g C m^{-2} and ranged from 0.14 in 2012 to 0.33 g C m^{-2} in 2016 during NGS (Fig. 6).

It is important to note that there was an extensive data gap in the EC measurements lasting from 22.9.2015 to 25.2.2016. The annual balance of 2016 was the highest in the whole study period (Fig. 5B): to confirm that this result was not affected by a long period of gap-filled data, I additionally calculated the annual balances by excluding the period of 1.1-25.2 (Appendix 1, Fig. A1). Since the year 2016 remained having the highest annual balance out of all years, I find evidence to conclude that the period with gap-filled data does not necessarily bias the results presented.

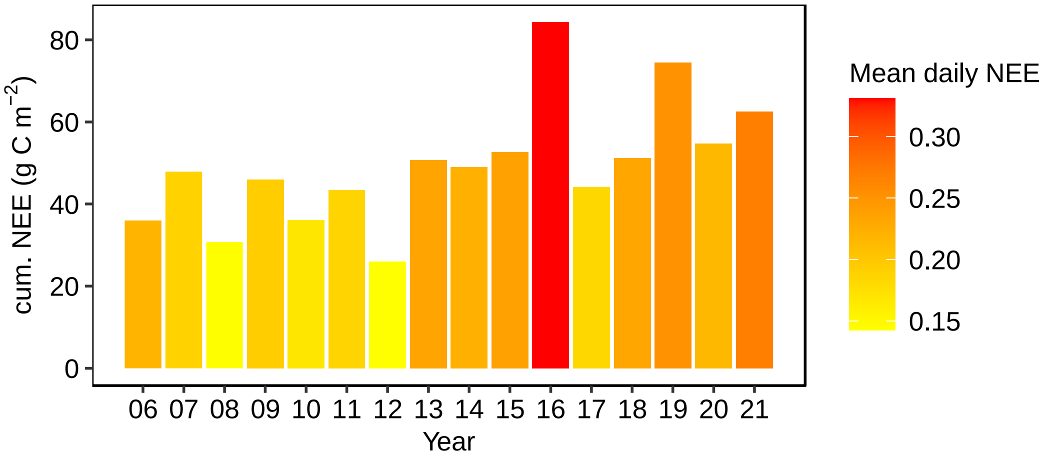

Figure 6. Cumulative CO_2 balance during NGS, aggregated to the year of the end of the NGS (e.g 2006 NGS refers the NGS that starts in autumn 2005 and ends in spring 2006). Colouring indicates the mean daily sum of NEE (unit: g C m^{-2} d^{-1}) during each NGS.

4.4 Variable importance controlling NEE

The random forest analysis isolated PAR and soil temperature as the most important variables driving NEE during GS, NGS and in the whole time period (annual, Fig. 7). Specifically, PAR had its highest importance during GS as expected, with a relative importance of 77% controlling NEE, whereas soil temperature was most important during NGS with a relative importance of 40% (Fig. 7). However, PAR was equally important during the NGS as soil temperature (Fig. 7). During the GS, soil temperature had only slightly higher relative importance (11%) compared to the other three variables (Fig. 7). At an annual scale, PAR had a relative importance of 61% over NEE, while soil temperature had a relative importance of 26%.

The three other covariates' (air temperature, VPD and WTD) relative importance were consistently lower compared to PAR and soil temperature (Fig 7.). Air temperature, VPD and WTD had their highest importance during NGS (Fig. 7). WTD had the highest relative importance after PAR and soil temperature with an importance of 10% during NGS (Fig. 7). The standard deviation was consistently low for all variables and during all seasons (less than 1 unit of percentage).

Including WTD as a covariate (Fig. 7 vs. Appendix 3, Fig. A3) resulted in a slight decrease in the relative importance of air temperature and VPD during GS, while increasing the importance of PAR, and slightly decreasing the importance of soil temperature during NGS.

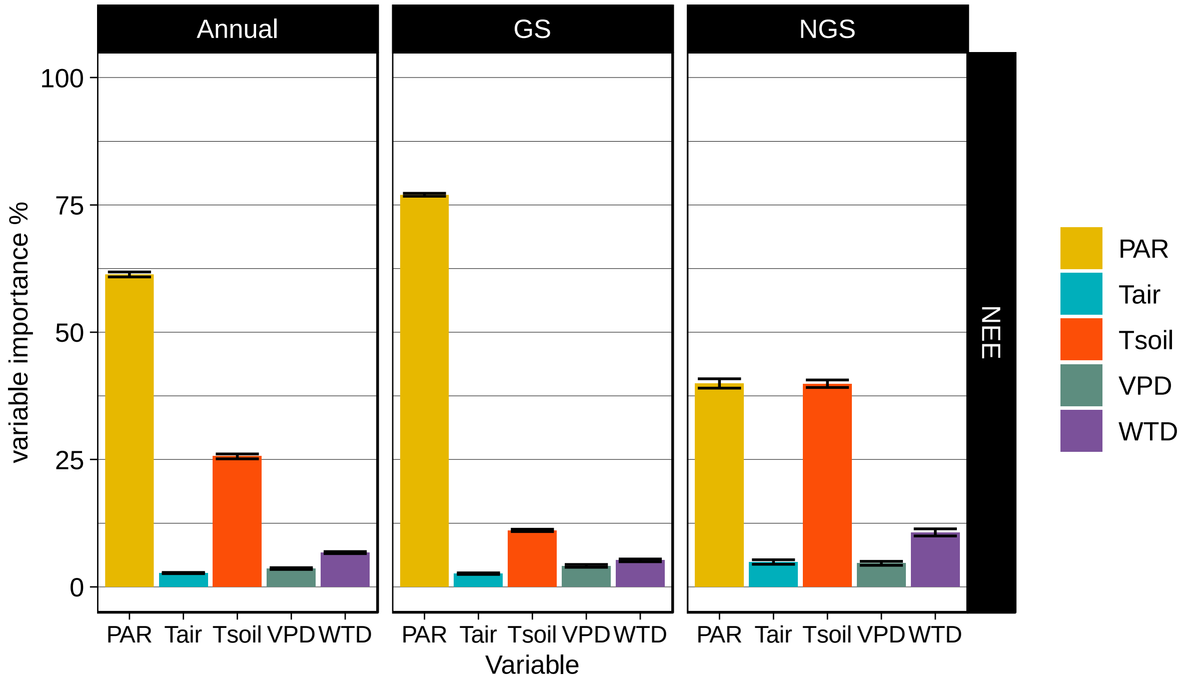

Figure 7. Relative importance of PAR, air temperature (Tair), soil temperature measured at 5 cm depth (Tsoil), vapor pressure deficit (VPD) and water table depth (WTD) to NEE in the whole time period of 2005-2021 (annual) and in GS and NGS.

4.5 Coherence between mean annual cycle of soil temperature and NEE

Mean NEE and soil temperature at 5 cm depth were coherent at the time-scale of 4 to 16 hours from mid-November to the end of March, and had a positive correlation between them (Fig. 8A). This means that the oscillations that happen on a 4 to 16 hour time-scale are correlating with each other. Soil temperature led NEE by 4 to 6 hours from June until September (Fig. 8), meaning that an increase in soil temperature was followed by an increase in NEE with a lag of 4 to 6 hours. The lag is the longest during peak of the growing season and then decreases towards November. The time series of NEE and soil temperature were generally more coherent with soil temperature measured at 5 cm depth (Fig. 8A) than at 50 cm depth (Fig. 8B). There was also coherence between soil temperature and NEE at around 500-1024 h (i.e., monthly) scale with negative correlation (Fig. 8A and Fig. 8B). This indicates that decreasing NEE is correlating with increasing soil temperature, as the soil temperature increases towards summer while simultaneously NEE decreases. There was no significant relationship between the mean annual cycle of NEE and soil temperature at either depth (5 or 50 cm) from mid-November to late March (Fig. 8A and Fig. 8B). This result may suggest two different things. First, a lack of a coherence between NEE and soil temperature during individual winters, which leads to incoherent relationship between the mean values. Second, high interannual variability in their measured values or in the lag between them during winter making the mean hourly values aggregated by yearly unable to capture the coherence between them.

A

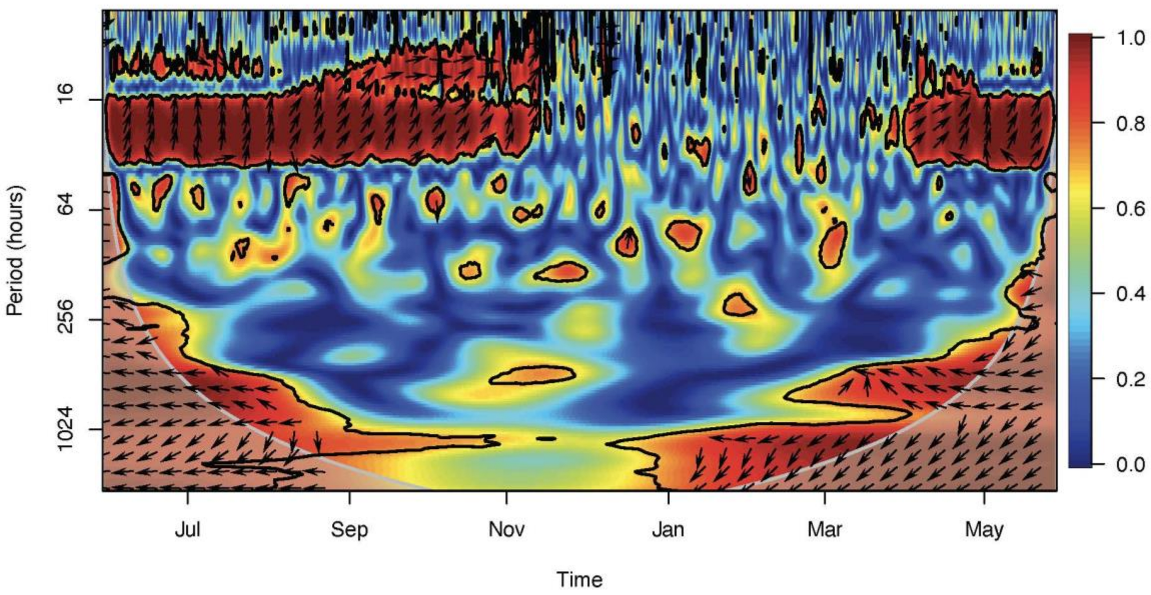

B

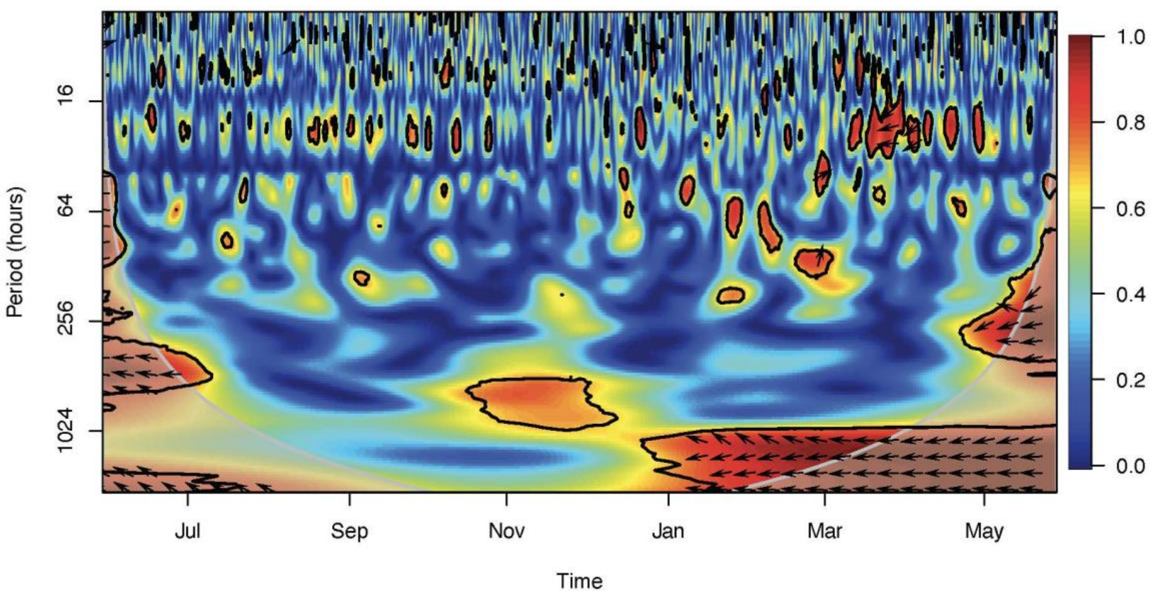

Figure 8. Wavelet coherence analysis between mean soil temperature measured at 5 cm (**A**) and 50 cm (**B**) depth and mean NEE from May 31st to next year's May 30th (Day of Year 150-149) for 2005-2021. Color represents the coherence from 0-1 at 0.05 level of significance. The arrows represent the phase status. Arrows pointing right indicate in-phase (positive correlation) and arrows pointing left indicate anti-phase (negative correlation) relationship. Arrows pointing up indicate that the soil temperature leads the NEE by a quarter cycle of the period. Arrows pointing down indicate that NEE leads soil temperature by a quarter cycle of the period. Grey contour indicates the cone of influence.

4.6 Respiration release in spring 2016

In April 2016 the ecosystem experienced a significant respiration release compared to the same months from any of the other 16 years in the dataset (Fig. 9). Such large carbon emission was large enough to shift the whole annual carbon balance from sink to net source of carbon to the atmosphere (Fig. 5B). The balance remained the highest during the whole time period even when calculated from the start of the true measurements on February 26th (Appendix 1, Fig. A1). NEE started increasing above average levels during the time of snow melt and peaked again when the surface layer started thawing (Fig. 9.).

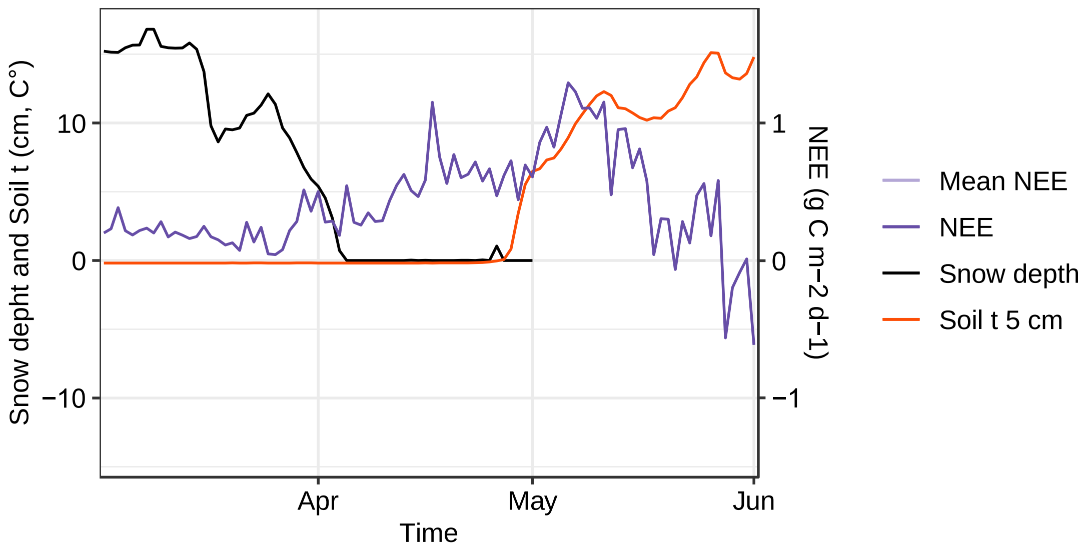

Figure 9. NEE, snow depth and soil temperature in March-June 2016 and the mean value of NEE in 2005-2021, excluding the year 2016. The two y axis have a different scale: left y axis for snow depth and soil temperature is multiplied by ten.

April and May cumulative emissions were large enough to offset the summer uptake in the following GS by 38%. The daily emissions (positive NEE) in April 2016 were nearly four-folded compared to the emissions in April on average, 0.53 and 0.133 g C d^{-1} m^{-2}, respectively (Fig. 10A). January 2016 had an extremely cold spell, resulting in the second coldest air temperature measured in 2005-2021, -25.15 ◦C (Fig. 10B). The air temperature dropped 30 ◦C in two weeks from late December to mid-January (Fig. 10B). The cold spell lasted for nearly three weeks. At Hyytiälä site located at 5 km from Siikaneva, there was no snowpack accumulated during the beginning of the cold spell. The snow depth increased from 0 to 4 cm during the cold spell, which was lower than the 2016-2021 average (16 cm). January was preceded by a warmer than average autumn, and before the cold spell, the air temperature had stayed mostly above freezing temperatures. The soil temperature at the surface dropped during the cold spell to the coldest measured in 2005-2021, and remained colder than average until mid-April, and similarly thawed later than average (Fig. 10C). In contrast, the soil was warmer than average at deeper (50cm) layers (Fig. 10D). The mean soil temperature at 50 cm for January to March was 0.85 ◦C higher than the mean for all Jan-March periods, 2.95 ◦C and 2.1 ◦C, respectively (Fig. 10D). However, wavelet coherence analysis revealed no coherence between the soil temperature at 50 cm depth and positive NEE during the time of respiration release or during the winter in general (Appendix 4, Fig. A4).

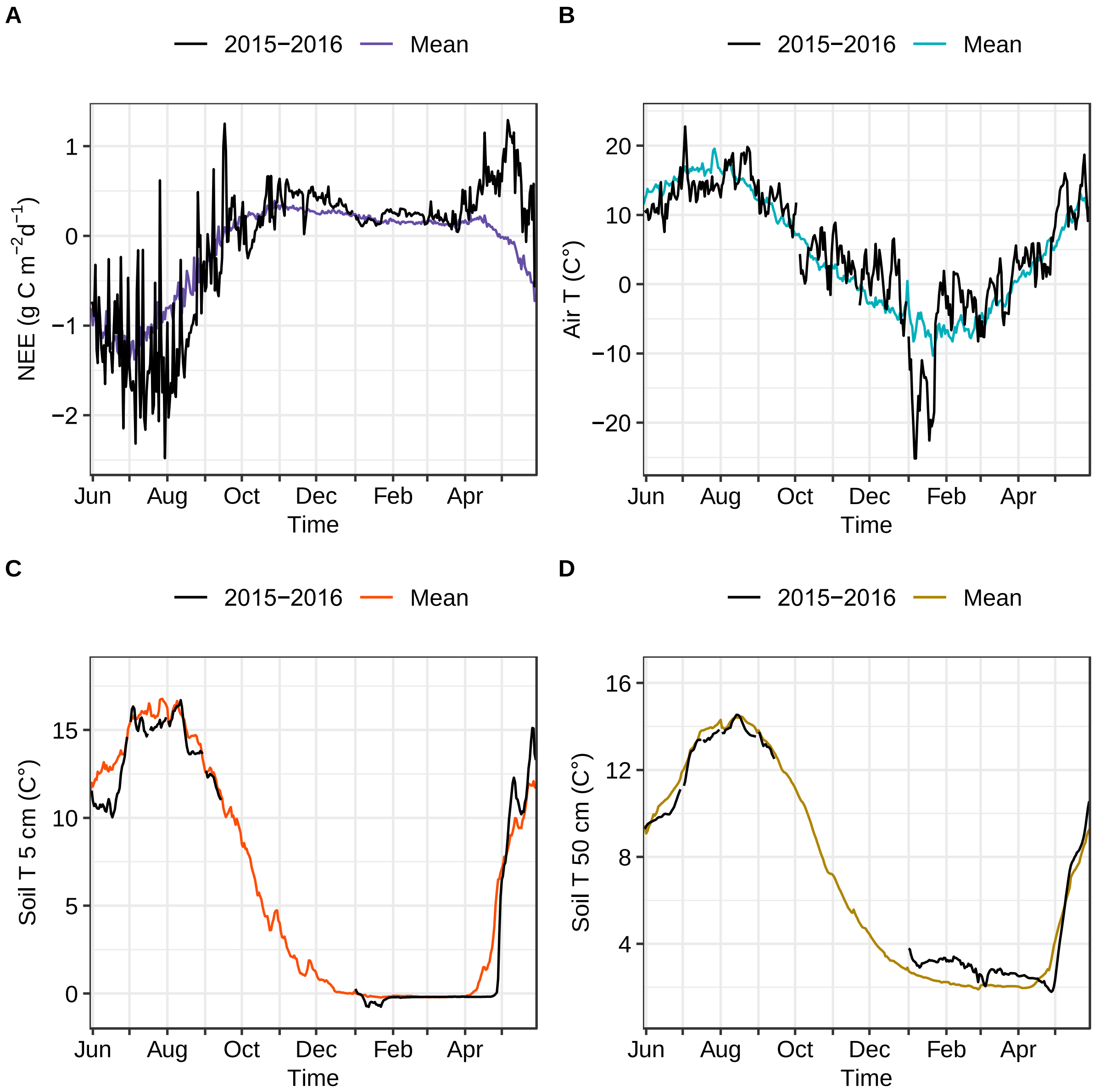

Figure 10. NEE (**A**), air temperature (**B**) and soil temperature at 5 cm depth (**C**) and 50 cm depth (**D**) from June to June in 2015-2016 (black line) and the mean (coloured lines) for 2005-2021, excluding the period from June to June in 2015-2016. Shading represents the standard error. Air temperature data is measured in Hyytiälä forestry site due to a gap of data in Siikaneva site in autumn 2015.

5 Discussion

The aim of this thesis was to analyze how much the NGS carbon balances accounts for the annual carbon balances, what is the relationship between soil temperature and NEE across different seasons, and how were the conditions in 2016 before and during the anomalous respiration release in spring.

5.1 Duration of NGS and contribution to the annual balance

The NGS accounted for 60% of the year in Siikaneva fen. On average, 222 days of the year was part of the NGS (Fig. 1), which is a similar duration compared to a more southern fen from Canada but at a climatically colder boreal zone (Cliche Trudeau et al., 2014), and two months less than the NGS at a more northern fen in Finland (Aurela et al., 2002). The CO_2 emissions during NGS offset (i.e., decrease) 57% of the carbon uptake in the following GS, similar in magnitude as in other studies covering boreal or arctic wetlands (Aurela et al., 2002; Wang et al., 2023; López-Blanco et al., 2018; Yao et al., 2022). The duration of NGS and average of daily fluxes during each NGS correlated with an equal power (correlation coefficient of 0.73 and 0.77, respectively) with the cumulative balances of NGS, suggesting that the interannual variation in the cumulative balances is both a result of processes affecting the duration of NGS (such as the onset of growing season) and the processes affecting the fluxes during the NGS (such as processes affecting microbial activity).

The fen ecosystem acted as a sink of CO_2 (-50.9 ± 39.4 g C m^{-2}) during most years, with the exception of 2016 and 2018 (Fig. 5B). In 2016, the positive annual carbon balance was caused by ecosystem processes during the NGS, specifically a respiration event that lasted around 6 weeks and occurred during the winter-spring transition period in Spring 2016 (Fig 9). Conversely, the positive carbon balance in 2018 was due to conditions during the GS, when a drought period in the summer of 2018 resulted in a weakened carbon sink strength during GS and an early onset of NGS (Rinne et al., 2020). The respiration release in 2016, despite being a shorter event than the dry summer of 2018, was significant enough to shift the entire annual balance to the positive CO_2 balance and to an even higher balance than that of 2018 (Fig. 5B).

5.2 Controlling variables on NEE across seasons

A random forest analysis was used to study the controlling variables (air and soil temperature, VPD, WTD, and PAR) on NEE between NGS, GS and a full-year cycle. Soil temperature was an important variable controlling the NEE of CO_2, and it had its highest importance during NGS (Fig. 7). This is not necessarily a novel result as such, but confirms that during NGS, soil temperature is one of the main controlling variables of the NGS fluxes. Moreover, due to its relatively high importance during the NGS, soil temperature was also the second most important variable on an annual scale (Fig. 7). This highlights the importance of NGS dynamics at a year-round scale with respect to carbon cycling dynamics. Soil temperature had higher importance than air temperature even during GS (Fig. 7), despite day-time air temperature being an important factor affecting photosynthesis at typical summer air temperatures in Siikaneva (Chapin et al. 2011, p. 147). The higher relative importance of soil temperature during the GS over air temperature could be explained by night-time respiration, since night-time fluxes are dominated by heterotrophic respiration. Part of the relative importance of soil temperature during GS could also be related to it cross-correlating with WTD. In fact, excluding WTD in the random forest analysis increased soil temperatures importance during NGS (Appendix 3, Figure A3.). This suggests that changes in WTD as driving force could be captured at some level by changes in soil temperature at 5 cm.

PAR was the most important driver across all seasons (Fig. 7), a result in line with previous studies (Lindroth et al., 2007; López-Blanco et al. 2017; Wei et al., 2022). The relatively high importance during NGS is likely explained by the definition used for seasons. Since the year was divided into only two seasons based on the sink activity, NGS can include some periods of the shoulder seasons when plants are still photosynthetically active, and thus driven by changes in PAR. Additionally, using hourly aggregated data emphasizes variables to which plants respond on a short time-scale, such as PAR (López-Blanco et al., 2017).

Many studies stress the crucial role that WTD has in wetland ecosystems on controlling NEE at various scales (e.g. Strachan et al., 2016; Peichl et al., 2014; Helfter et al., 2015). In this study, WTD was the third most important variable, and had lower importance than soil temperature during GS (Fig. 7). Similarly, Bubier et al. (1998) found that soil temperature at 5 cm explained ecosystem respiration the best and including water table depth to the analysis increased the explanatory power of the analysis only slightly.

Generally, these results confirm the importance of PAR and soil temperature controlling hourly aggregated NEE. These variables are typically used in partitioning NEE into GPP and Reco (e.g Kulmala et al., 2019). However, in Siikaneva wetland, NEE is partitioned with using air temperature in the respiration function. Interestingly this result highlights the potential uncertainties that using air temperature could introduce to the calculation of Reco gross fluxes, since air temperature showed a consistently lower importance compared to soil temperature.

5.3 Degree of coherence between the mean annual cycle of soil temperature and NEE

Wavelet coherence analysis was used to study if the average annual cycle of NEE and soil temperature were coherent and whether there was a systematic lag between them. Despite soil temperature being a weaker driver for NEE during GS than NGS (Fig. 7), the wavelet analysis suggests a significant pattern of positive correlation between soil temperature (at 5 cm depth) and NEE in their mean annual cycle only during April to mid-November (Fig. 8A), therefore suggesting no coherence during most of the NGS.

During April to mid-November, NEE and soil temperature at 5 cm were positively correlated (Fig 8A). Additionally, the coherence analysis suggests a consistent lag with soil temperature leading NEE for most of the summer (Fig 8A). This coherent relationship indicates that the oscillations at a timescale of 4-16 hours (i.e., at a diurnal cycle) were consistent and coherent enough between the different years for the mean values to capture it. Positive correlation means that increasing soil temperature was associated to an increase in NEE, meaning that increasing soil temperature likely promoted respiration. Additionally, the lag was consistent enough to be captured by the mean values, suggesting that it is a consistent feature in their relationship. Similar results of a coherence between surface soil temperature and NEE during summer where soil temperature leads NEE has been found at wetland site in Tibetan plateau by Yao et al (2022).

Soil temperature at 50 cm depth was significantly less coherent with NEE compared to the surface temperature (Fig. 8B). Similarly, Bubier et al., (1998) found that ecosystem respiration was better explained by temperature at a 5 cm depth than by warming at deeper soil layers. However, since during winter the surface of the soil is colder than the deeper soil layers (Fig. 3), the heterotrophic respiration could take place at those deeper layers rather than at the surface (Aurela et al., 2002). Despite that, there was no coherence between NEE and soil temperature at 50 cm depth during winter (Fig. 8B)

The period with no coherence between the NEE and soil temperature at 5 cm depth lasted from mid-November to end of March. The timing of the incoherent relationship takes mostly place during NGS, since on average NGS lasted from September 17^{th} to April 29^{th} (Fig. 1). This lack of coherence between the mean annual cycles does not mean that there would not be a significant relationship during individual years. For instance, the data was aggregated by combining all years together to create a mean hourly value for each hour of each day of the year (DoY 1-365). The mean values of NEE and soil temperature represent the general fluctuation (e.g. on a diurnal and annual scale) in both time series and thus they capture only reoccurring trends. In fact, the period with incoherent relationship coincides with the period when the NEE has no clear diurnal pattern, since according to Rinne et al. (2018), at Siikaneva fen the CO_2 fluxes have a clear diurnal cycle from to mid-April to mid-October. This could suggest that the daily cycle is the only feature that is temporally consistent enough to be picked up by the data aggregation used. Processes during NGS that would affect soil temperature and potentially NEE (like e.g snow melt) are maybe not temporally consistent enough to be clearly reflected in the mean annual cycles. Different data aggregation (e.g using daily mean values instead of hourly values or using the full time series instead of mean values) could reveal more efficiently the level of coherence during individual years.

Even though soil temperature was not found to be a strong driver during GS periods (with a relative importance of 11%, see Fig. 7), the wavelet coherence analysis suggests that the coherence between them is consistent (Fig. 8A). In fact, the consistent lag between these two variables could suggest that the random forest analysis underestimates the relative importance of the soil temperature since it does not consider the lag when assessing the importance. Therefore, the two methods are complementary to each other since random forest analysis assesses the hierarchy between the covariates and wavelet analysis expands the analysis to a wider temporal scale.

5.4 The respiration release in Spring 2016 was likely enhanced by the conditions in the previous winter

An anomalously high emissions of CO_2 were measured in April and May in 2016 (Fig. 9), large enough to turn the whole year's carbon balance to positive (Fig. 5B). This period with anomalous respiration offset 38% of the carbon uptake of the following GS. This finding is consistent in magnitude with previously studied spring-time pulses of CO_2 (e.g Raz-Yaseef et al., 2017; Sullivan et al., 2012; Arndt et al., 2020; Wang et al., 2023). However, the duration of the respiration event is longer than the ones observed at other sites, and NEE data shows more of a gradual increase rather than a pulse-like behavior (Fig 9).

It is worth pointing that across the winter period in 2016 there was a change in instrumentation that caused a long gap in the measurements. The measurements started again on the 26^{th} of February, and there were approximately six weeks of measurements before the observed CO_2 pulse. The data went through regular quality screening processes before and during the pulse with no signs of instrument malfunction (Pasi Kolari, personal communication). The annual balance remained anomalously high even when calculated from the start of the true measurements in February (Appendix 1, Fig. A1).

Spring-time CO_2 pulses can result from wintertime emissions that have accumulated in the soil or snow and have been retained there due to snowpack or ice acting as a lid on top of the soil surface (Sullivan et al., 2012). During snowmelt and soil thawing periods, these emissions can burst from the soil into the atmosphere, causing a pulse increasing emissions (Raz-Yaseef et al., 2017; Arndt et al., 2020). At Siikaneva fen, the soil was anomalously warm at a depth of 50 cm, which could have promoted higher-than-average respiration throughout the winter (Fig 10D). However, wavelet coherence analysis did not reveal a significant relationship between the soil temperature at 50 cm depth and the respiration release in April 2016 (Appendix 4, Fig A4). This result could be due to the different periodicity of temperature fluctuations in the soil and the respiration event in the spring. Although the wavelet analysis identifies relationships between the two time series and can quantify the temporal lag between them, the coherence is analyzed at the same timescale. Thus, it would not likely pick up a significant relationship with soil temperature and a sudden, pulse-like increase in NEE, if the soil temperature does not have a similar pulse-like fluctuation of similar duration. An ice cap could have contributed to the accumulation of CO_2 in the soil (Martz et al., 2016; Morgner et al., 2010). Unfortunately, there were no direct measurements or observations to confirm the presence of a layer of ice on top of the soil, but the conditions were favourable for it. Since before the cold spell the air temperature stayed mostly above 0 ◦C (Fig. 10B) it is likely that a large portion of the precipitation came down as water, allowing the cold spell in January to create an ice lid on top of the wet soil since there was no snow to insulate the surface from the cold air.

An undetermined part of the respiration observed in April during snowmelt and soil thawing periods could be derived from wintertime respiration retained in the soil. However, there are also other ecosystem processes that could have boosted the respiration during soil thawing periods. For example, soil freeze-up could have created mechanical disturbance and break down biomass in the soil, which could promote faster decomposition in the following spring (Brooks et al., 2005; Byun et al., 2021.). Freezing and thawing can lyse the winter microbial populations, which releases easily degradable carbon and nutrients to the surviving community, boosting respiration post thaw (Brooks et al., 2005). The year 2016 was preceded by 3 years when the soil temperature stayed below 0 ◦C for a relatively short periods (Fig. 4), potentially stressing the impact of what the record-cold soil surface might have had to the microbial communities. The melting snow can additionally promote respiration, when the oxygen-rich snowmelt water brings oxygen to the deeper layers of soil (Arndt et al., 2020), which, together with increasing soil temperature and available carbon and nutrient creates a favourable environment for microbial activity.

The spring-time pulses of CO_2 are an unknown part of the boreal and arctic carbon budget, but as growing evidence shows, they can significantly alter the sink capacity of these ecosystems. Therefore, it is crucial to understand the potential mechanisms behind them to reliably assess the future climate forcing's impact to the carbon sink strength of arctic and boreal wetlands.

6 Conclusions

Full-year NEE of CO_2 and particularly wintertime fluxes are less studied compared to carbon cycling dynamics during summer and growing seasons (GS). In this study, I analyzed the non-growing season (NGS) fluxes of a boreal wetland in Siikaneva. NGS CO_2 balance was a significant component of the annual carbon balance in this fen system, offsetting nearly 60% of the following GS's carbon sink. Full-year observations are therefore crucial for reliable estimations on the sink potential of northern ecosystems. CO_2 exchange during NGS was driven by PAR and soil temperature. The relatively high percentage of importance of PAR was likely due to the presence of some parts of the shoulder seasons in the NGS. This further highlights the importance of studying these transition periods between summer and winter in more detail. The mean annual cycles of NEE and soil temperature were not coherent during the winter months, likely due to the lack of a clear diurnal cycle in NEE and thus high interannual variability in their values. This stresses the importance of studying the coherence during and across individual years. Since soil temperature was a key driver during NGS, it is crucial to understand what drives its variability, such as the timing, thickness, and duration of snow cover. Additionally, the winter-spring transition periods can contribute greatly to the annual balance through periods of high of respiration, as observed in Siikaneva in Spring 2016 during snowmelt and soil thaw periods. A six-week period in April and May shifted the whole annual carbon balance of 2016 to a net source of CO_2, leading to the highest positive carbon balance during the whole study period. A cold spell during January preceding a warm autumn created a drastic temperature profile in the soil column with the coldest temperatures in the whole study period measured at the surface, while the deeper layers stayed warmer than average throughout the winter. This thesis shows evidence that the variability of soil temperature can influence or trigger respiration pulses such as the one documented 2016. Continuous year-round measurements are thus needed to identify such possible non-trivial carry-over effect across seasons.

References

Aanderud, Z. T., Jones, S. E., Schoolmaster, D. R., Fierer, N., & Lennon, J. T. (2013). Sensitivity of soil respiration and microbial communities to altered snowfall. *Soil Biology and Biochemistry*, *57*, 217–227.

AMAP, 2021. AMAP Arctic Climate Change Update 2021: Key Trends and Impacts. Arctic Monitoring and Assessment Programme (AMAP), Tromsø, Norway.

Arndt, K. A., Lipson, D. A., Hashemi, J., Oechel, W. C., & Zona, D. (2020). Snow melt stimulates ecosystem respiration in Arctic ecosystems. *Global Change Biology*, *26*(9), 5042–5051.

Arora, V. K., Katavouta, A., Williams, R. G., Jones, C. D., Brovkin, V., Friedlingstein, P., Schwinger, J., Bopp, L., Boucher, O., Cadule, P., Chamberlain, M. A., Christian, J. R., Delire, C., Fisher, R. A., Hajima, T., Ilyina, T., Joetzjer, E., Kawamiya, M., Koven, C. D., … Ziehn, T. (2020). Carbon–concentration and carbon–climate feedbacks in CMIP6 models and their comparison to CMIP5 models. *Biogeosciences*, *17*(16), 4173–4222.

Aubinet, M., Vesala, T., & Papale, D. (Eds.). (2012). *Eddy covariance: a practical guide to measurement and data analysis*. Springer Science & Business Media.

Auguie B. (2017). gridExtra: Miscellaneous Functions for "Grid" Graphics. R package version 2.3.

Aurela, M., Laurila, T., & Tuovinen, J.-P. (2002). Annual CO2 balance of a subarctic fen in northern Europe: Importance of the wintertime efflux. *Journal of Geophysical Research: Atmospheres*, *107*(D21), ACH 17-1-ACH 17-12.

Aurela, M., Laurila, T., & Tuovinen, J.-P. (2004). The timing of snow melt controls the annual CO2 balance in a subarctic fen. *Geophysical Research Letters*, *31*(16). L16119.

Aurela, M., Riutta, T., Laurila, T., Tuovinen, J.-P., Vesala, T., Tuittila, E.-S., Rinne, J., Haapanala, S., & Laine, J. (2007). CO2 exchange of a sedge fen in southern Finland—The impact of a drought period. *Tellus B*, *59*(5), 826–837.

Aurela, M., Lohila, A., Tuovinen, J.-P., Hatakka, J., Riutta, T. & Laurila, T. (2009). Carbon dioxide exchange on a northern boreal fen. *Boreal Environmental research. 14.* 699–710.

Baldocchi, D. D. (2003). Assessing the eddy covariance technique for evaluating carbon dioxide exchange rates of ecosystems: Past, present and future: CARBON BALANCE and EDDY COVARIANCE. *Global Change Biology*, *9*(4), 479–492.

Bond-Lamberty, B., Bailey, V. L., Chen, M., Gough, C. M., & Vargas, R. (2018). Globally rising soil heterotrophic respiration over recent decades. *Nature*, *560*(7716), 80-83.

Bradford, M. A., Wieder, W. R., Bonan, G. B., Fierer, N., Raymond, P. A., & Crowther, T. W. (2016). Managing uncertainty in soil carbon feedbacks to climate change. *Nature Climate Change*, *6*(8), 751–758.

Breiman, L. (2001). Random Forests. *Machine Learning*, *45*(1), 5–32.

Brooks, P. D., McKnight, D., & Elder, K. (2005). Carbon limitation of soil respiration under winter snowpacks: Potential feedbacks between growing season and winter carbon fluxes. *Global Change Biology, 11(2),* 231–238.

Bubier, J. L., Crill, P. M., Moore, T. R., Savage, K., & Varner, R. K. (1998). Seasonal patterns and controls on net ecosystem CO2 exchange in a boreal peatland complex. *Global Biogeochemical Cycles*, *12*(4), 703–714.

Byun, E., Rezanezhad, F., Fairbairn, L., Slowinski, S., Basiliko, N., Price, J. S., Quinton, W. L., Roy-Léveillée, P., Webster, K., & Van Cappellen, P. (2021). Temperature, moisture and freeze–thaw controls on CO2 production in soil incubations from northern peatlands. *Scientific Reports*, *11*(1), 1–15.

Böttcher, K., Aurela, M., Kervinen, M., Markkanen, T., Mattila, O.-P., Kolari, P., Metsämäki, S., Aalto, T., Arslan, A. N., & Pulliainen, J. (2014). MODIS time-series-derived indicators for the beginning of the growing season in boreal coniferous forest—A comparison with CO2 flux measurements and phenological observations in Finland. *Remote Sensing of Environment*, *140*, 625–638.

Cliche Trudeau, N., Garneau, M., & Pelletier, L. (2014). Interannual variability in the CO2 balance of a boreal patterned fen, James Bay, Canada. *Biogeochemistry*, *118*(1), 371–387.

Curiel Yuste, J., Baldocchi, D. D., Gershenson, A., Goldstein, A., Misson, L., & Wong, S. (2007). Microbial soil respiration and its dependency on carbon inputs, soil temperature and moisture. *Global Change Biology*, *13*(9), 2018–2035.

Chapin, F. S., Matson, P. A., & Vitousek, P. M. (2011). *Principles of Terrestrial Ecosystem Ecology*. Springer.

Drebs, A., Nordlund, A., Karlsson, P., Helminen, J. and Rissanen, P. 2002. Climatological statistics of Finland 1971-2000. Finnish Meteorological Institute.

Frey, S. D., Lee, J., Melillo, J. M., & Six, J. (2013). The temperature response of soil microbial efficiency and its feedback to climate. *Nature Climate Change*, *3*(4), 395–398.

Friedlingstein, P., O'Sullivan, M., Jones, M. W., Andrew, R. M., Gregor, L., Hauck, J., Le Quéré, C., Luijkx, I. T., Olsen, A., Peters, G. P., Peters, W., Pongratz, J., Schwingshackl, C., Sitch, S., Canadell, J. G., Ciais, P., Jackson, R. B., Alin, S. R., Alkama, R., … Zheng, B. (2022). Global Carbon Budget 2022. *Earth System Science Data*, *14*(11), 4811–4900.

Gorham, E. (1991). Northern Peatlands: Role in the Carbon Cycle and Probable Responses to Climatic Warming. *Ecological Applications*, *1(2)*. 182-195.

Grinsted, A., Moore, J. C., & Jevrejeva, S. (2004). Application of the cross wavelet transform and wavelet coherence to geophysical time series. *Nonlinear Processes in Geophysics, 11*(5/6), 561–566.

Groffman, P. M., Driscoll, C. T., Fahey, T. J., Hardy, J. P., Fitzhugh, R. D., & Tierney, G. L. (2001). Colder soils in a warmer world: A snow manipulation study in a northern hardwood forest ecosystem. *Biogeochemistry*, *56*(2), 135–150.

Harris, C.R., Millman, K.J., van der Walt, S.J. (2020) Array programming with NumPy. *Nature, 585,* 357–362.

Helfter, C., Campbell, C., Dinsmore, K. J., Drewer, J., Coyle, M., Anderson, M., Skiba, U., Nemitz, E., Billett, M. F., & Sutton, M. A. (2015). Drivers of long-term variability in CO_2 net ecosystem exchange in a temperate peatland. *Biogeosciences*, *12*(6), 1799–1811.

Hunter J.D. (2007). Matplotlib: A 2D Graphics Environment. *Computing in Science & Engineering, 9(3),* 90-95.

IPCC, 2022: *Climate Change 2022: Impacts, Adaptation, and Vulnerability.* Contribution of Working Group II to the Sixth Assessment Report of the Intergovernmental Panel on Climate Change [H.-O. Pörtner, D.C. Roberts, M. Tignor, E.S. Poloczanska, K. Mintenbeck, A. Alegría, M. Craig, S. Langsdorf, S. Löschke, V. Möller, A. Okem, B. Rama (eds.)]. Cambridge University Press.

Kulmala, L., Pumpanen, J., Kolari, P., Dengel, S., Berninger, F., Köster, K., Matkala, L., Vanhatalo, A., Vesala, T., & Bäck, J. (2019). Inter- and intra-annual dynamics of photosynthesis differ between forest floor vegetation and tree canopy in a subarctic Scots pine stand. *Agricultural and Forest Meteorology*, *271*, 1–11.

Li, Q., Leroy, F., Zocatelli, R., Gogo, S., Jacotot, A., Guimbaud, C., & Laggoun-Défarge, F. (2021). Abiotic and biotic drivers of microbial respiration in peat and its sensitivity to temperature change. *Soil Biology and Biochemistry*, *153*, 108077.

Lindroth, A., Lund, M., Nilsson, M., Aurela, M., Christensen, T. R., Laurila, T., Rinne, J., Riutta, T., Sagerfors, J., StröM, L., Tuovinen, J.-P., & Vesala, T. (2007). Environmental controls on the CO2 exchange in north European mires. *Tellus B: Chemical and Physical Meteorology*, *59*(5), 812–825.

López-Blanco, E., Lund, M., Christensen, T. R., Tamstorf, M. P., Smallman, T. L., Slevin, D., Westergaard-Nielsen, A., Hansen, B. U., Abermann, J., & Williams, M. (2018). Plant Traits are Key Determinants in Buffering the Meteorological Sensitivity of Net Carbon Exchanges of Arctic Tundra. *Journal of Geophysical Research: Biogeosciences*, *123*(9), 2675–2694.

López-Blanco, E., Lund, M., Williams, M., Tamstorf, M. P., Westergaard-Nielsen, A., Exbrayat, J.-F., Hansen, B. U., & Christensen, T. R. (2017). Exchange of CO_2 in Arctic tundra: Impacts of meteorological variations and biological disturbance. *Biogeosciences*, *14*(19), 4467–4483.

Martz, F., Vuosku, J., Ovaskainen, A., Stark, S., & Rautio, P. (2016). The Snow Must Go On: Ground Ice Encasement, Snow Compaction and Absence of Snow Differently Cause Soil Hypoxia, CO2 Accumulation and Tree Seedling Damage in Boreal Forest. *PLoS ONE*, *11*(6), e0156620.

Mastepanov, M., Sigsgaard, C., Tagesson, T., Ström, L., Tamstorf, M. P., Lund, M., & Christensen, T. R. (2013). Revisiting factors controlling methane emissions from high-Arctic tundra. *Biogeosciences*, *10*(7), 5139–5158.

Mikkonen, S., Laine, M., Mäkelä, H. M., Gregow, H., Tuomenvirta, H., Lahtinen, M., & Laaksonen, A. (2015). Trends in the average temperature in Finland, 1847–2013. *Stochastic Environmental Research and Risk Assessment*, *29*(6), 1521–1529.

Morgner, E., Elberling, B., Strebel, D., & Cooper, E. J. (2010). The importance of winter in annual ecosystem respiration in the High Arctic: Effects of snow depth in two vegetation types. *Polar Research*, *29*(1), 58-74.

Moritz S., Bartz-Beielstein T. (2017). imputeTS: Time Series Missing Value Imputation in R. *The RJournal, 9(1),* 207-218.

Natali, S. M., Watts, J. D., Rogers, B. M., Potter, S., Ludwig, S. M., Selbmann, A.-K., Sullivan, P. F., Abbott, B. W., Arndt, K. A., Birch, L., Björkman, M. P., Bloom, A. A., Celis, G., Christensen, T. R., Christiansen, C. T., Commane, R., Cooper, E. J., Crill, P., Czimczik, C., … Zona, D. (2019). Large loss of CO2 in winter observed across the northern permafrost region. *Nature Climate Change*, *9*(11), 852–857.

Nichols, J. E., & Peteet, D. M. (2019). Rapid expansion of northern peatlands and doubled estimate of carbon storage. *Nature Geoscience*, *12*(11), 917–921.

Panikov, N. S., Flanagan, P. W., Oechel, W. C., Mastepanov, M. A., & Christensen, T. R. (2006). Microbial activity in soils frozen to below −39°C. *Soil Biology and Biochemistry*, *38*(4), 785–794.

Pedregosa, F., Varoquaux, G., Gramfort, A., Michel, V., Thirion, B., Grisel, O., ... & Duchesnay, E. (2011). Scikit-learn: Machine learning in Python. *the Journal of machine Learning research*, *12*, 2825-2830.

Peichl, M., Öquist, M., Ottosson Löfvenius, M., Ilstedt, U., Sagerfors, J., Grelle, A., Lindroth, A., & Nilsson, M. B. (2014). A 12-year record reveals pre-growing season temperature and water table level threshold effects on the net carbon dioxide exchange in a boreal fen. *Environmental Research Letters*, *9*(5), 055006.

Qian, B., Gregorich, E. G., Gameda, S., Hopkins, D. W., & Wang, X. L. (2011). Observed soil temperature trends associated with climate change in Canada. *Journal of Geophysical Research: Atmospheres*, *116*(D2). D02106.

Rafat, A., Byun, E., Rezanezhad, F., Quinton, W. L., Humphreys, E. R., Webster, K., & Cappellen, P. V. (2022). The definition of the non-growing season matters: A case study of net ecosystem carbon exchange from a Canadian peatland. *Environmental Research Communications*, *4*(2), 021003.

Rantanen, M., Karpechko, A. Y., Lipponen, A., Nordling, K., Hyvärinen, O., Ruosteenoja, K., Vihma, T., & Laaksonen, A. (2022). The Arctic has warmed nearly four times faster than the globe since 1979. *Communications Earth & Environment*, *3*(1).

Raz-Yaseef, N., Torn, M. S., Wu, Y., Billesbach, D. P., Liljedahl, A. K., Kneafsey, T. J., Romanovsky, V. E., Cook, D. R., & Wullschleger, S. D. (2017). Large CO2 and CH4 emissions from polygonal tundra during spring thaw in northern Alaska. *Geophysical Research Letters*, *44*(1), 504–513.

Rinne, J., Riutta, T., Pihlatie, M., Aurela, M., Haapanala, S., Tuovinen, J.-P., Tuittila, E.-S., & Vesala, T. (2007). Annual cycle of methane emission from a boreal fen measured by the eddy covariance technique. *Tellus B*, *59*(3), 449–457.

Rinne, J., Tuittila, E.-S., Peltola, O., Li, X., Raivonen, M., Alekseychik, P., Haapanala, S., Pihlatie, M., Aurela, M., Mammarella, I., & Vesala, T. (2018). Temporal Variation of Ecosystem Scale Methane Emission From a Boreal Fen in Relation to Temperature, Water Table Position, and Carbon Dioxide Fluxes. *Global Biogeochemical Cycles*, *32*(7), 1087–1106.

Rinne, J., Tuovinen, J.-P., Klemedtsson, L., Aurela, M., Holst, J., Lohila, A., Weslien, P., Vestin, P., Łakomiec, P., Peichl, M., Tuittila, E.-S., Heiskanen, L., Laurila, T., Li, X., Alekseychik, P., Mammarella, I., Ström, L., Crill, P., & Nilsson, M. B. (2020). Effect of the 2018 European drought on methane and carbon dioxide exchange of northern mire ecosystems. *Philosophical Transactions of the Royal Society B: Biological Sciences*, *375*(1810), 20190517.

Rudd, D. A., Karami, M., & Fensholt, R. (2021). Towards High-Resolution Land-Cover Classification of Greenland: A Case Study Covering Kobbefjord, Disko and Zackenberg. *Remote Sensing*, *13*(18), 3559.

Schimel, J. P., & Clein, J. S. (1996). Microbial response to freeze-thaw cycles in tundra and taiga soils. *Soil Biology and Biochemistry*, *28*(8), 1061–1066.

Strachan, I. B., Pelletier, L., & Bonneville, M.-C. (2016). Inter-annual variability in water table depth controls net ecosystem carbon dioxide exchange in a boreal bog. *Biogeochemistry*, *127*(1), 99–111.

Sullivan, B. W., Dore, S., Montes-Helu, M. C., Kolb, T. E., & Hart, S. C. (2012). Pulse Emissions of Carbon Dioxide during Snowmelt at a High-Elevation Site in Northern Arizona, U.S.A. *Arctic, Antarctic, and Alpine Research*, *44*(2), 247–254.

Tarik C. Gouhier, Aslak Grinsted, Viliam Simko (2021). R package biwavelet: Conduct Univariate and Bivariate Wavelet Analyses (Version 0.20.21).

Virkkala, A.-M., Natali, S. M., Rogers, B. M., Watts, J. D., Savage, K., Connon, S. J., Mauritz, M., Schuur, E. A. G., Peter, D., Minions, C., Nojeim, J., Commane, R., Emmerton, C. A., Goeckede, M., Helbig, M., Holl, D., Iwata, H., Kobayashi, H., Kolari, P., … Zyryanov, V. I. (2022). The ABCflux database: Arctic–boreal CO2 flux observations and ancillary information aggregated to monthly time steps across terrestrial ecosystems. *Earth System Science Data*, *14*(1), 179–208.

Wang, H., Yu, L., Chen, L., Zhang, Z., Li, X., Liang, N., Peng, C., & He, J.-S. (2023). Carbon fluxes and soil carbon dynamics along a gradient of biogeomorphic succession in alpine wetlands of Tibetan Plateau. *Fundamental Research*, *3*(2), 151–159.

Warner, D. L., Bond-Lamberty, B., Jian, J., Stell, E., & Vargas, R. (2019). Spatial Predictions and Associated Uncertainty of Annual Soil Respiration at the Global Scale. *Global Biogeochemical Cycles*, *33*(12), 1733–1745.

Wickham, H. (2016). ggplot2: Elegant Graphics for Data Analysis. Springer-Verlag New York.

Wickham H., François R., Henry L. and Müller K. (2021). dplyr: A Grammar of Data Manipulation. R package version 1.0.7.

Wei, J., Li, X., Liu, L., Christensen, T. R., Jiang, Z., Ma, Y., Wu, X., Yao, H., & López-Blanco, E. (2022). Radiation, soil water content, and temperature effects on carbon cycling in an alpine swamp meadow of the northeastern Qinghai–Tibetan Plateau. *Biogeosciences*, *19*(3), 861–875.

Wutzler T., Reichstein M., Moffat A.M., and Migliavacca M. (2022). REddyProc: Post Processing of (Half-)Hourly Eddy-Covariance Measurements. R package version 1.3.2.

Yao, H., Peng, H., Hong, B., Guo, Q., Ding, H., Hong, Y., Zhu, Y., Cai, C., & Chi, J. (2022). Environmental Controls on Multi-Scale Dynamics of Net Carbon Dioxide Exchange From an Alpine Peatland on the Eastern Qinghai-Tibet Plateau. *Frontiers in Plant Science*, *12*, 791343.

Yu, H., Luedeling, E., & Xu, J. (2010). Winter and spring warming result in delayed spring phenology on the Tibetan Plateau. *Proceedings of the National Academy of Sciences*, *107*(51), 22151–22156.

Yu, Z., Beilman, D. W., Frolking, S., MacDonald, G. M., Roulet, N. T., Camill, P., & Charman, D. J. (2011). Peatlands and Their Role in the Global Carbon Cycle. *Eos, Transactions American Geophysical Union*, *92*(12), 97–98.

Zhang, T. (2005). Influence of the seasonal snow cover on the ground thermal regime: An overview. *Reviews of Geophysics*, *43*(4). RG4002.

Appendix

Appendix 1 Cumulative annual CO_2 balance excluding DoY 0-50

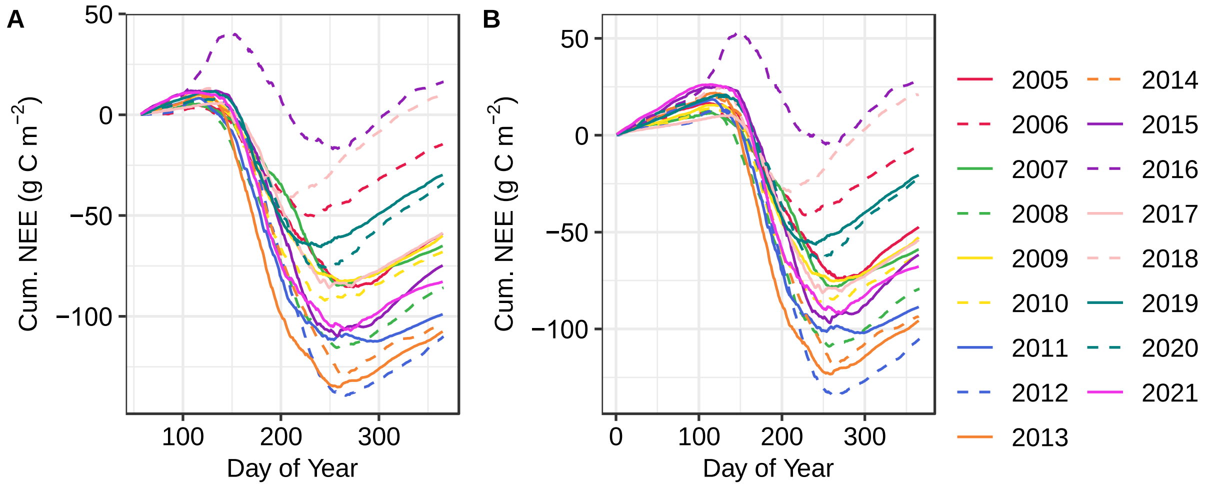

Figure A1. Cumulative sums of gap-filled NEE for starting from DoY 57 (**A**) and starting from DoY 1 (**B**). Daily sums are calculated from hourly averaged data.

Appendix 2 Gap-filled soil temperature at 50 depth depth in 2016

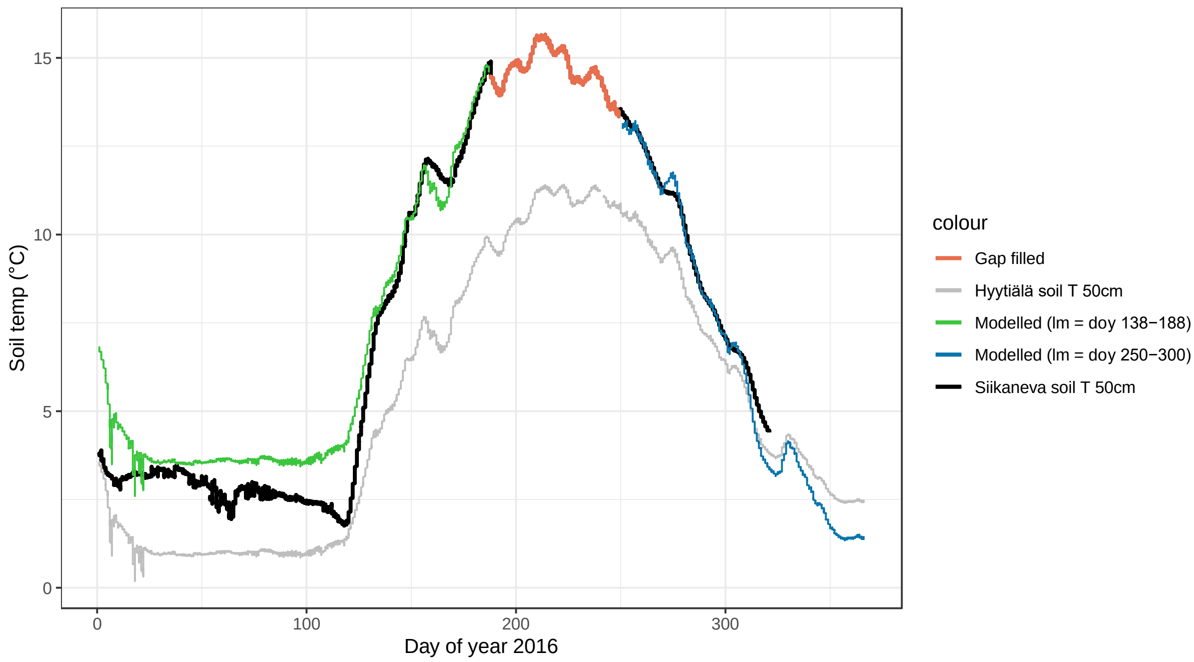

Figure A2. Soil temperature at 50 cm depth in 2016 in Siikaneva (black line) and Hyytiälä site (grey line), the modelled soil temperature for Siikaneva site by using two models (green and blue line), and the final gap-filled soil temperature (pink line) The green line shows the modelled soil temperature when using a linear regression model that is trained with soil temperature data from Hyytiälä and Siikaneva from DoY 138-188. The blue line shows a modelled soil temperature of a similar model but that is trained with data from DoY 250-300. The final gap-filled values are obtained from using a transition function that changes incrementally from using the function obtained from the model before the gap to the function obtained from the model after the gap.

Appendix 3 Random forest analysis excluding WTD

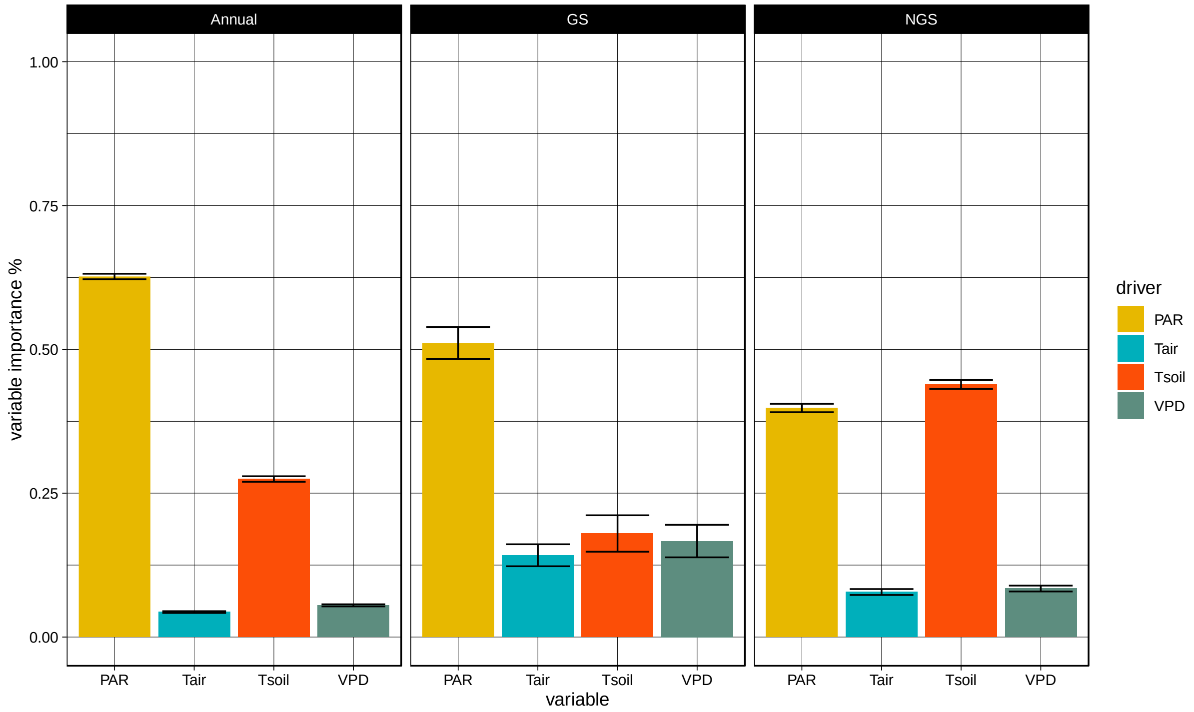

Figure A3. Relative importance of PAR, air temperature (Tair), soil temperature measured at 5 cm depth (Tsoil) and VPD to NEE in the whole time period of 2005-2021 (annual) and in GS and NGS.

Appendix 4 Coherence between soil temperature at 50 cm depth and NEE in 2016

A

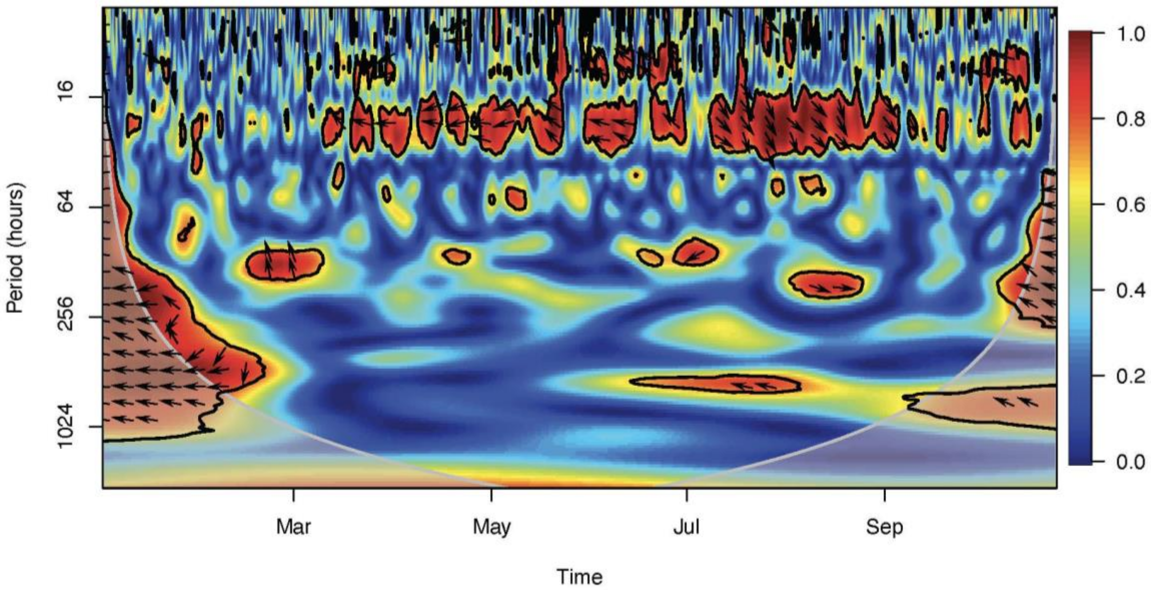

B

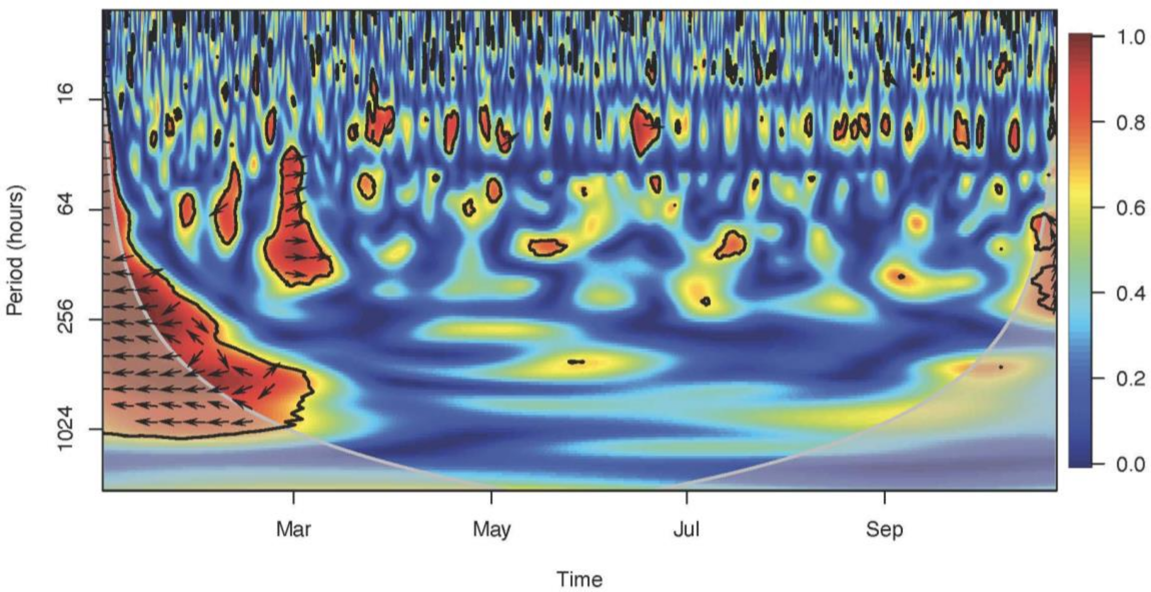

Figure A4: Wavelet coherence analysis between soil temperature measured at 50 cm depth and NEE from Jan 1st to Oct 27th (Day of Year 1-300) in 2016 (**A**) and mean values for whole time period 2005-2021 excluding 2016 (**B**). Colour represents the coherence from 0-1 at 0.05 level of significance. The arrows represent the phase status. Arrows pointing right indicate in-phase (positive correlation) and arrows pointing left indicate anti-phase (negative correlation) relationship. Arrows pointing up indicate that the soil temperature leads the NEE by a quarter cycle of the period. Arrows pointing down indicate that NEE leads soil temperature by a quarter cycle of the period. Grey contour indicates the cone of influence.